AMERICAN SOCIETY FOR MICROBIOLOGY | Journal of Virology®

CELLULAR RESPONSE TO INFECTION

Potent *In Vivo* NK Cell-Mediated Elimination of HIV-1-Infected Cells Mobilized by a gp120-Bispecific and Hexavalent Broadly Neutralizing Fusion Protein

Ariola Bardhi,[a] Yanling Wu,[b] Weizao Chen,[c] Wei Li,[c] Zhongyu Zhu,[c] Jian Hua Zheng,[a] Hing Wong,[d] Emily Jeng,[d] Jennifer Jones,[e] Christina Ochsenbauer,[e] John C. Kappes,[e,f] Dimiter S. Dimitrov,[c] Tianlei Ying,[b] Harris Goldstein[a]

Departments of Microbiology and Immunology and Pediatrics, Albert Einstein College of Medicine, Bronx, New York, USA[a]; Key Laboratory of Medical Molecular Virology of Ministries of Education and Health, School of Basic Medical Sciences, Fudan University, Shanghai, China[b]; Protein Interactions Section, Cancer and Inflammation Program, Center for Cancer Research, National Cancer Institute, National Institutes of Health, Frederick, Maryland, USA[c]; Altor BioScience Corporation, Miramar, Florida, USA[d]; Department of Medicine, University of Alabama at Birmingham, Birmingham, Alabama, USA[e]; Birmingham Veterans Affairs Medical Center, Research Service, Birmingham, Alabama, USA[f]

ABSTRACT Antibodies bound to human immunodeficiency virus type 1 (HIV-1) envelope protein expressed by infected cells mobilize antibody-dependent cellular cytotoxicity (ADCC) to eliminate the HIV-1-infected cells and thereby suppress HIV-1 infection and delay disease progression. Studies treating HIV-1-infected individuals with latency reactivation agents to reduce their latent HIV-1 reservoirs indicated that their HIV-1-specific immune responses were insufficient to effectively eliminate the reactivated latent HIV-1-infected T cells. Mobilization of ADCC may facilitate elimination of reactivated latent HIV-1-infected cells to deplete the HIV-1 reservoir and contribute to a functional HIV-1 cure. The most effective antibodies for controlling and eradicating HIV-1 infection would likely have the dual capacities of potently neutralizing a broad range of HIV-1 isolates and effectively mobilizing HIV-1-specific ADCC to eliminate HIV-1-infected cells. For this purpose, we constructed LSEVh-LS-F, a broadly neutralizing, defucosylated hexavalent fusion protein specific for both the CD4 and coreceptor gp120-binding sites. LSEVh-LS-F potently inhibited *in vivo* HIV-1 and simian-human immunodeficiency virus (SHIV) infection in humanized mouse and macaque models, respectively, including *in vivo* neutralization of HIV-1 strains resistant to the broadly neutralizing antibodies VRC01 and 3BNC117. We developed a novel humanized mouse model to evaluate *in vivo* human NK cell-mediated elimination of HIV-1-infected cells by ADCC and utilized it to demonstrate that LSEVh-LS-F rapidly mobilized NK cells to eliminate >80% of HIV-1-infected cells *in vivo* 1 day after its administration. The capacity of LSEVh-LS-F to eliminate HIV-1-infected cells via ADCC combined with its broad neutralization activity supports its potential use as an immunotherapeutic agent to eliminate reactivated latent cells and deplete the HIV-1 reservoir.

IMPORTANCE Mobilization of antibody-dependent cellular cytotoxicity (ADCC) to eliminate reactivated latent HIV-1-infected cells is a strategy which may contribute to depleting the HIV-1 reservoir and achieving a functional HIV-1 cure. To more effectively mobilize ADCC, we designed and constructed LSEVh-LS-F, a broadly neutralizing, defucosylated hexavalent fusion protein specific for both the CD4 and coreceptor gp120-binding sites. LSEVh-LS-F potently inhibited *in vivo* HIV-1 and SHIV

Received 6 June 2017 **Accepted** 31 July 2017

Accepted manuscript posted online 9 August 2017

Citation Bardhi A, Wu Y, Chen W, Li W, Zhu Z, Zheng JH, Wong H, Jeng E, Jones J, Ochsenbauer C, Kappes JC, Dimitrov DS, Ying T, Goldstein H. 2017. Potent *in vivo* NK cell-mediated elimination of HIV-1-infected cells mobilized by a gp120-bispecific and hexavalent broadly neutralizing fusion protein. J Virol 91:e00937-17. https://doi.org/10.1128/JVI.00937-17.

Editor Guido Silvestri, Emory University

Address correspondence to Harris Goldstein, harris.goldstein@einstein.yu.edu.

infection in humanized mouse and macaque models, respectively, including *in vivo* neutralization of an HIV-1 strain resistant to the broadly neutralizing antibodies VRC01 and 3BNC117. Using a novel humanized mouse model, we demonstrated that LSEVh-LS-F rapidly mobilized NK cells to eliminate >80% of HIV-1-infected cells *in vivo* 1 day after its administration. The capacity of LSEVh-LS-F to eliminate HIV-1-infected cells via ADCC combined with its broad neutralization activity supports its potential use as an immunotherapeutic agent to eliminate reactivated latent cells and deplete the HIV-1 reservoir.

KEYWORDS NK cell, human immunodeficiency virus

Binding to the human immunodeficiency virus type 1 (HIV-1) envelope and neutralizing viral infectivity by preventing viral entry and the subsequent infection of cells constitute the major mechanism utilized by broadly neutralizing antibodies (bNAb) to control HIV-1 infection (1). Antibodies can also utilize another mechanism to inhibit HIV-1 infection, antibody-dependent cellular cytotoxicity (ADCC), which is mediated by their binding to HIV-1 envelope molecules expressed on the surface of infected cells and utilization of their constant (Fc) domains to recruit FcγRIIIa-expressing effector cells, such as NK cells, to kill the infected cells (2). ADCC-mediated elimination of reactivated latent HIV-1-infected cells is a potential mechanism by which antibodies can markedly reduce the HIV-1 reservoir and contribute to a functional cure (3). It is likely that the most effective therapeutic antibodies for treating HIV-1-infected individuals are bNAb with the dual capacity to potently neutralize a broad range of HIV-1 isolates and effectively mobilize HIV-1-specific ADCC to eliminate HIV-1-infected cells, including reactivated latent infected cells (4). However, despite the capacity of potent bNAb, such as VRC01 and 3BNC117, to neutralize up to 90% of HIV-1 isolates tested (5), markedly suppress HIV-1 viremia after infusion into HIV-1-infected patients (6), and eliminate HIV-1-infected cells by ADCC (4), the rapid emergence and expansion of bNAb-resistant HIV-1 during bNAb monotherapy (6, 7) limits the efficacy of bNAb monotherapy (8, 9) and would likely also limit their capacity to mobilize ADCC. To overcome this limitation and prevent or delay the *in vivo* emergence of bNAb-resistant HIV-1 (5), we developed a bispecific hexavalent CD4-antibody fusion protein, 4Dm2m, composed of two engineered domains, mD1.22 and m36.4, each specific for a different neutralizing gp120 epitope. mD1.22, an engineered mutant of the D1 extracellular domain of CD4, selectively binds to the gp120 CD4-binding site (10), while m36.4, an antibody domain, targets the highly conserved CD4-induced (CD4i) gp120 coreceptor-binding site (11). Because CD4 binding to gp120 induces full exposure of the m36.4-targetted gp120 epitope, the linkage in 4Dm2m of the soluble one-domain CD4, mD1.22, to the m36.4 domain greatly augments the binding and neutralizing activity of m36.4 (10). 4Dm2m is a bispecific hexavalent fusion protein consisting of four mD1.22 molecules and two m36.4 molecules linked to a heavy-chain constant domain 1 (CH1), a kappa light-chain constant domain (CK), and an IgG1 Fc domain (10). The potential for hexavalent binding of 4Dm2m to gp120 increases its avidity for gp120 and enables it to neutralize HIV-1 ~10-fold more potently than the native bNAb, VRC01 (10). Furthermore, the bispecific binding of 4Dm2m to two independent gp120 epitopes should constrain the *in vivo* emergence of 4Dm2m-resistant HIV-1 by requiring independent mutations at each targeted site, as reported for combination bNAb treatment (5). Finally, because mD1.22 was designed to mirror the CD4 structure, mutations in gp120 which reduce mD1.22 binding should be paralleled by decreased CD4 binding, which would diminish HIV-1 replicative capacity and thereby inhibit the emergence of mD1.22 escape mutations. We generated a structural variant of 4Dm2m, LSEVh-LS, with a significantly increased *in vivo* half-life due to its improved structural stability and increased binding to the FcRn (12). We further augmented the capacity of LSEVh-LS to mobilize ADCC activity by defucosylating its Fc domain to increase its affinity for FcγRIIIa and thereby amplify its ability to recruit effector cells (13). In the current study, we examined the *in vitro* and *in vivo* anti-HIV-1 activities of the defucosylated LSEVh-LS, named LSEVh-LS-F, and

demonstrated that LSEVh-LS-F potently inhibited *in vitro* and *in vivo* infection by VRC01- and 3BNC117-resistant HIV-1 strains and effectively mobilized NK cell-mediated ADCC activity to eliminate HIV-1-infected cells in humanized mice. LSEVh-LS-F also significantly suppressed acute simian-human immunodeficiency virus (SHIV) infection of rhesus macaques. These findings support the potential contribution of LSEVh-LS-F to treatment regimens aimed at reducing or eradicating the reservoir of HIV-1-infected cells.

RESULTS

LSEVh-LS-F potently neutralizes VRC01-susceptible and VRC01-resistant strains of HIV-1 *in vitro* in human peripheral blood mononuclear cells (PBMC). We previously engineered an exceptionally potent and broadly neutralizing CD4-antibody fusion protein, LSEVh-LS (12), composed of a human CD4 domain, mD1.22, and a human antibody domain, m36.4, each specific for a different neutralizing gp120 epitope (Fig. 1A). Defucosylation of the Fc domains of antibodies increases their affinity toward FcγRIIIa expressed by NK cells and macrophages and thereby significantly amplifies their capacity to mediate ADCC (14, 15) and eliminate tumor cells in cancer patients (16–18). To enhance the capacity of LSEVh-LS to mobilize ADCC and eliminate HIV-1-infected cells, we produced defucosylated LSEVh-LS-F in GDP-fucose transporter (GFT) gene-inactivated CHO cells (CHO-F6) as described previously (19). The defucosylation of LSEVh-LS-F was confirmed by high-resolution mass spectrometry (MS) analysis, which demonstrated a marked reduction in the deconvoluted mass of LSEVh-LS-F compared with LSEVh-LS (Fig. 1B) and a 7.5-fold increase in the affinity of LSEVh-LS-F to FcγRIIIa (equilibrium dissociation constant [K_D] = 65 nM) compared to that of LSEVh-LS (K_D = 490 nM) (Fig. 1C).

We investigated whether the bispecific hexavalent structure of LSEVh-LS-F increases its capacity to bind to gp120 molecules expressed on the surface of infected cells and mediate ADCC by evaluating the dose-response binding of LSEVh-LS-F to HIV-1 Env protein expressed on the surface of activated ACH-2 cells, a latently infected T cell line used as a model of HIV-1 latency (20). Flow cytometric analysis of activated ACH-2 cells stained with LSEVh-LS-F or VRC01 indicated that at all doses evaluated, LSEVh-LS-F displayed increased binding to the Env trimer expressed on the surface of activated ACH-2 cells compared to VRC01 (Fig. 2A). To evaluate the capacity of LSEVh-LS-F and the original fusion protein construct, 4Dm2m, to neutralize bNAb-resistant HIV-1 in comparison to VRC01, we examined their capacity to inhibit the infection of PBMC by different HIV-1_{Env}-LucR viruses which were isogenic except for the expression of different Env genes, including some which are moderately (C.Du151.2; 50% inhibitory concentration [IC_{50}], 3.2 μg/ml) or highly (45_01E11 and C.Du172.17; IC_{50}, >50 μg/ml) resistant to neutralization by VRC01 (21, 22), or highly resistant (C.Du422.1; IC_{50}, >50 μg/ml) to neutralization by both VRC01 and 3BNC117 (23, 24). Two days after activated PBMC were infected with the indicated HIV-1_{Env}-LucR and cultured with added LSEVh-LS-F, 4Dm2m, or VRC01, HIV-1 infection was quantified by measuring *Renilla reniformis* luciferase (LucR) activity in cell lysates. LSEVh-LS-F and 4Dm2m displayed similar to slightly better neutralization of VRC01-sensitive viruses compared to that of VRC01 (Fig. 2B). In contrast, the capacity of LSEVh-LS-F and 4Dm2m to suppress infection with HIV-1 expressing VRC01-resistant Env was greater than 100-fold more than that of VRC01, including potent suppression of HIV-1 expressing C.Du422.1 Env, a strain resistant to neutralization by VRC01 and 3BNC117, and HIV-1 expressing 45_01E11 Env, a strain completely resistant to VRC01 neutralization (Fig. 2C). We examined the capacity of LSEVh-LS-F to mediate ADCC activity using as effector cells Jurkat T-NFAT-Luc2-CD16A cells (Jurkat T-CD16A cells), which activate a nuclear factor of activated T cell response element (NFAT-RE)-regulated luciferase reporter gene after FcγRIIIa engagement by antibody bound to target cells (25). Jurkat T-CD16A cells were incubated overnight with the indicated concentration of LSEVh-LS-F and either no target cells, CHO cells, or CHO cells stably expressing a clade-B HIV-1 Env (CHO-gp160SC cells). LSEVh-LS-F displayed dose-responsive ADCC activity as indicated by FcγRIIIa engagement and activation of

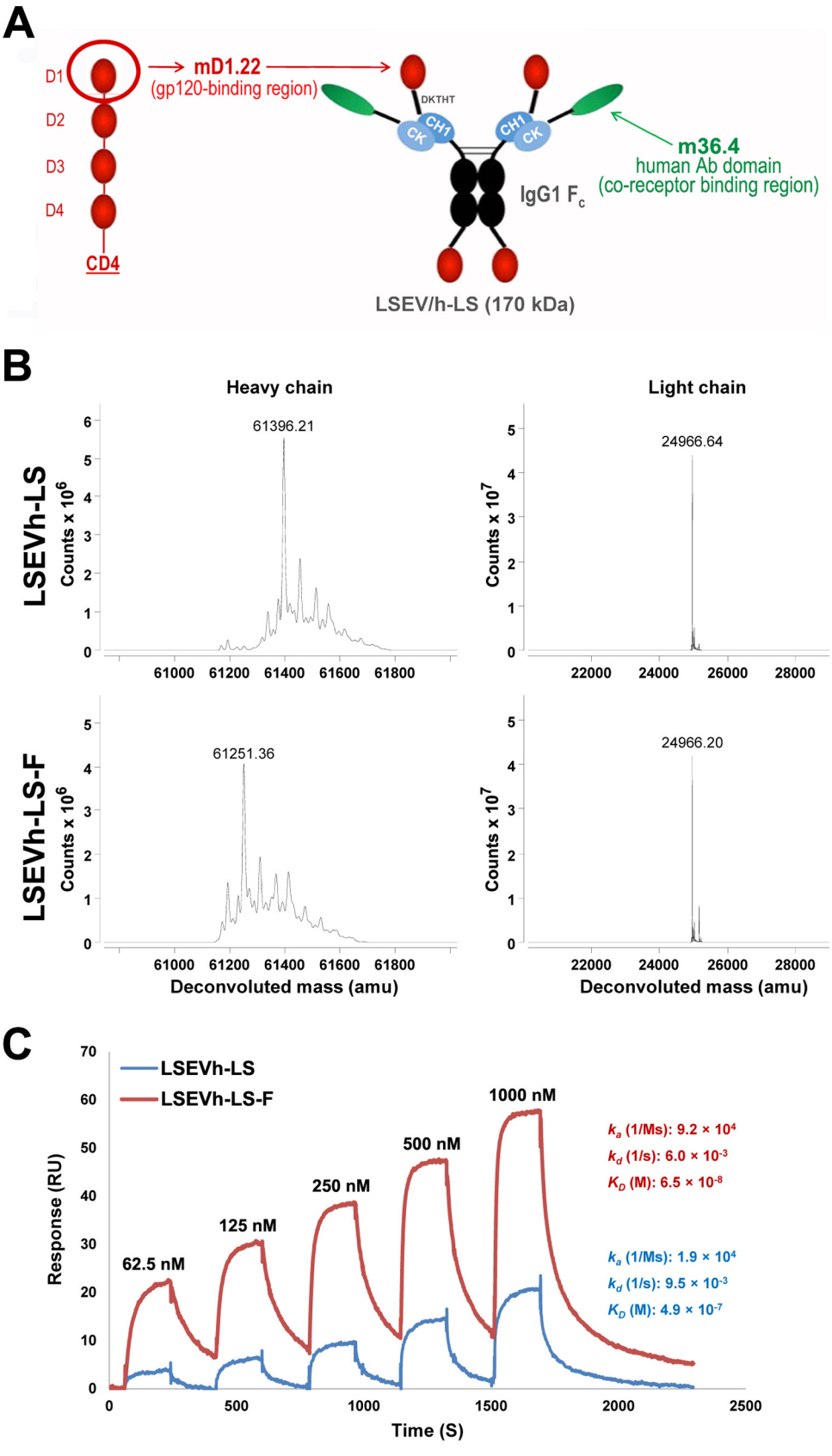

FIG 1 Structure, mass spectrometry analysis, and binding kinetics. (A) Schematic representation of LSEVh-LS expressing mD1.22 and m36.4. IgG1 Fc, human IgG1 crystallizable fragment; CH1, human IgG1 heavy-chain constant region 1; CK, human antibody kappa light-chain constant region; DKTHT, linker sequence derived from the

(Continued on next page)

the luciferase reporter gene after incubation with CHO-gp160SC cells but not with CHO cells (Fig. 2D).

LSEVh-LS-F potently inhibits *in vivo* HIV-1 infection in hu-spl-PBMC-NSG mice. We previously developed a humanized mouse model to evaluate the *in vivo* capacity of human NK cells activated by an interleukin-15 (IL-15) superagonist complex (IL-15SA/ALT-803) to inhibit HIV-1 infection, which was constructed by intrasplenically injecting immunodeficient NOD-SCID-IL-2r$\gamma^{-/-}$ (NSG) mice with activated human PBMC (hu-spl-PBMC-NSG mice) (26). The activated human PBMC, which include $CD4^+$ T cells and NK cells, persist in the mouse spleens for at least 1 month after intrasplenic injection, become infected after intrasplenic HIV-1 inoculation, and should support HIV-1-specific ADCC activity (26). During the week after intrasplenic injection of hu-spl-PBMC-NSG mice with HIV-1_{Env}-LucR, there is rapid expansion of the number of HIV-1-infected cells in the mouse spleens, which can be visualized by sequential IVIS imaging of untreated hu-spl-PBMC-NSG mice (Fig. 3A). As the first step of using these mice to evaluate the *in vivo* anti-HIV-1 activity of LSEVh-LS-F, we compared the *in vivo* pharmacokinetics of LSEVh-LS-F and VRC01 in NSG mice. By 3 days after intravenous injection, LSEVh-LS-F serum levels were less than 5% of VRC01 serum levels but were still above the 80% inhibitory concentration (IC_{80}) for VRC01-susceptible HIV-1-Env strains such as JR-CSF(Fig. 3B). To investigate the capacity of LSEVh-LS-F to inhibit *in vivo* infection by VRC01-resistant HIV-1, we challenged hu-spl-PBMC-NSG mice either with VRC01/3BNC117-sensitive (HIV-$1_{JR\text{-}CSF}$-LucR) or with VRC01/3BNC117-resistant (HIV-$1_{c.Du422.1}$-LucR) viruses. One day later, groups of mice were either left untreated or intravenously injected with LSEVh-LS-F, VRC01, or an isotype control monoclonal antibody (MAb). Five days later, HIV-1 infection was evaluated by measuring LucR activity in splenic lysates. Both LSEVh-LS-F and VRC01 potently suppressed infection of the VRC01/3BNC117-sensitive HIV-1_{JRCSF}-LucR virus (Fig. 3C). In contrast, despite the 20-fold-higher serum levels of VRC01 than of LSEVh-LS-F (Fig. 3B), LSEVh-LS-F more significantly ($P < 0.05$) inhibited infection with the VRC01/3BNC117-resistant strain HIV-$1_{C.Du422.1}$-LucR than VRC01 (Fig. 3D).

LSEVh-LS-F eliminates HIV-1-infected cells by an NK cell-mediated mechanism. We adapted the hu-spl-PBMC-NSG mice to be used as a novel *in vivo* model for evaluating HIV-1-specific ADCC activity to investigate the *in vivo* capacity of defucosylated LSEVh-LS-F to eliminate HIV-1-infected cells. hu-spl-PBMC-NSG mice were infected by intrasplenic injection with HIV-1_{JRCSF}-LucR. Five days later, after *in vivo* infection was established, mice were either left untreated or treated with LSEVh-LS-F, VRC01, or an isotype control MAb. Because full HIV-1 replication in primary T cells takes at least 24 h (27), we posited that the reduction in LucR activity measured 1 day after treatment should indicate the elimination of HIV-1-infected cells by ADCC. One day after HIV-1_{JRCSF}-LucR-infected hu-spl-PBMC-NSG mice were treated with LSEVh-LS-F, the number of HIV-1-infected cells in the mouse spleens, as indicated by LucR activity, was reduced by almost 90% compared to that after treatment with the control MAb, which was 2-fold greater ($P < 0.01$) than the ~40% reduction mediated by VRC01 treatment (Fig. 4A). *In vivo* visualization of productively infected cells by IVIS imaging demonstrated a marked reduction in LucR activity in the spleens of hu-spl-PBMC-NSG mice treated with LSEVh-LS-F compared to the spleens of untreated hu-spl-PBMC-NSG mice (Fig. 4B). To

FIG 1 Legend (Continued)
human IgG1 hinge. The calculated molecular mass is shown in parentheses. (B) High-resolution mass spectrometry analysis of LSEVh-LS produced in 293-F cells, which was designated LSEVh-LS, and LSEVh-LS produced in GFT gene knockout CHOF6 cells, which was designated LSEVh-LS-F. Mass spectra were shown, with deconvoluted mass for the major peak indicated at the top. G0, Fc oligosaccharides without galactose and fucose; G0F, Fc oligosaccharides without galactose but with fucose. (C) Binding kinetics of LSEVh-LS and LSEVh-LS-F with recombinant human FcγRIIIa as measured by SPR. SPR analysis was performed on Biacore X100 by using a single-cycle approach according to the manufacturer's instructions. Analytes were tested at 1000, 500, 250, 125, and 62.5 nM concentrations. The kinetic constants shown on the right were calculated from the sensograms fitted with monovalent binding model of the BiacoreX100 evaluation software 2.0. k_a, association rate constant; k_d, dissociation rate constant; K_D, equilibrium dissociation constant.

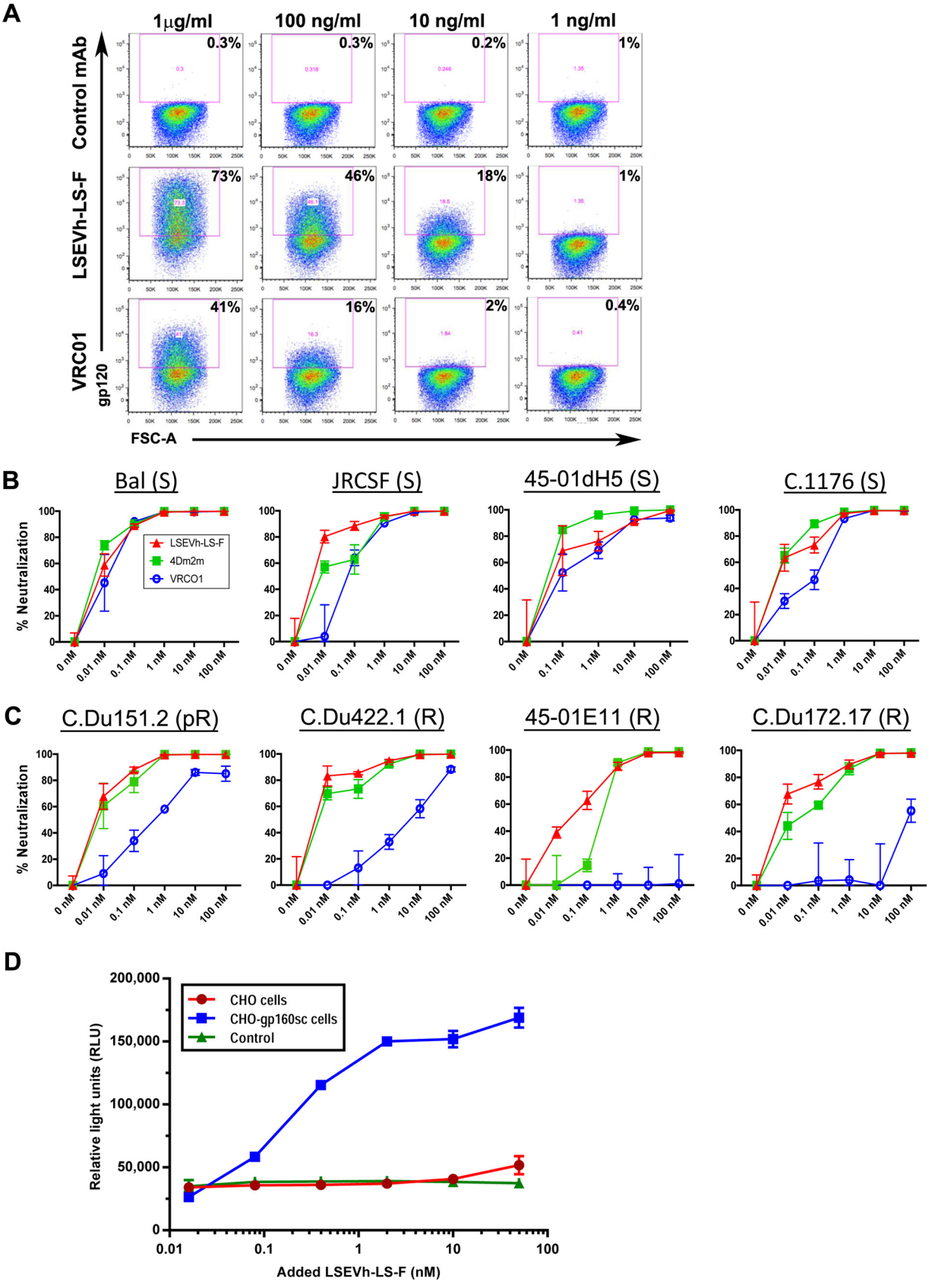

FIG 2 LSEVh-LS-F and VRC01 binding to Env expressed on the surface of ACH-2 cells, *in vitro* neutralizing activity, and LSEVh-LS-F *in vitro* ADCC activity. (A) Unactivated ACH-2 cells and PMA-activated ACH2 cells were stained with the indicated concentration of biotinylated anti-Ebola virus

(Continued on next page)

confirm that the LSEVh-LS-F-mediated reduction in HIV-1 infection was a consequence of NK cell-mediated ADCC (28), we depleted the NK cell population from the PBMC prior to their injection into hu-spl-PBMC-NSG mice and examined whether this would abrogate LSEVh-LS-F activity. NSG mice were intrasplenically injected with either unfractionated PBMC or NK cell-depleted PBMC and intrasplenically infected with HIV-1_{JRCSF}-LucR. Five days later the humanized mice were either left untreated or treated with LSEVh-LS-F, and 1 day later, HIV-1 infection in the spleens was quantified by measuring LucR activity. As described above, LSEVh-LS-F treatment markedly reduced HIV-1 infection by >70% in the spleens of NSG mice constructed by intrasplenic injection of unfractionated PBMC. In contrast, LSEVh-LS-F treatment did not decrease HIV-1 infection in the spleens of NSG mice intrasplenically injected with NK cell-depleted PBMC (Fig. 5A).

Activation of NK cells can increase their capacity to mediate ADCC. For example, the ADCC-mediated *in vivo* elimination of human B cell lymphoma cells via NK cells recruited by anti-CD20 MAb was significantly increased by NK cell activation with IL-15SA (ALT-803), a bivalent IL-15Rα–Fc fusion protein binding two mutant IL-15 molecules (29). We previously demonstrated that *in vivo* IL-15SA treatment of hu-spl-PBMC-NSG mice activates the human NK cells populating the mouse spleen and enables them to potently reduce intrasplenic HIV-1 infection (26). To determine whether activation of NK cells by IL-15SA increased LSEVh-LS-F-mediated depletion of HIV-1-infected cells, we infected hu-spl-PBMC-NSG mice with HIV-1_{JRCSF}-LucR and 5 days later either did not treat the mice or treated the mice with IL-15SA, LSEVh-LS-F, or a combination of both. For these experiments, we reduced the treatment dose of LSEVh-LS-F by half to enable us to identify the additive effect of IL-15SA treatment on the LSEVh-LS-F-mediated depletion of HIV-1-infected cells. The combination of LSEVh-LS-F and IL-15SA reduced HIV-1_{JRCSF}-LucR infection by 80%, 2-fold more than treatment with either LSEVh-LS-F or IL-15SA alone (Fig. 5B). Taken together, these results demonstrate that the bispecific hexavalent antibody LSEVh-LS-F potently inhibited HIV-1 infection, as well as markedly reduced established HIV-1 infection via NK cell-dependent ADCC, which could be further enhanced by IL-15SA activation of NK cells.

LSEVh-LS-F potently inhibits SHIV infection in macaques. To examine the capacity of LSEVh-LS-F to inhibit acute SHIV infection of rhesus macaques, 7 days after infection with $SHIV_{SF162P3}$ and prior to the onset of peak viremia, we injected them with either LSEVh-LS-F (10 mg/kg) or phosphate-buffered saline (PBS). SHIV RNA in plasma was measured at the indicated times (Fig. 6A). PBS-treated animals reached the peak of infection on average at day 9 after infection, which was suppressed by LSEVh-LS-F treatment on day 7 (Fig. 6B). A well-recognized limitation of macaque studies involves the cost and logistic factors that limit the number of animals available for inclusion in each experimental group. When the number of animals in each group is relatively small, as in the case of the present study, and variations are large, which is typical for macaques, a significant quantitative effect may not be identified by direct statistical comparison with a control group. Individual variations of viremia were seen in each macaque. Therefore, to evaluate the statistical significance of the difference between treated and untreated macaques, we normalized the virus RNA by dividing by the value of virus RNA at day 7 and subtracting 1. The administration of LSEVh-LS-F at day 7

FIG 2 Legend (Continued)
MAb (control), VRC01, or LSEVh-LS-F, followed by incubation with streptavidin-PE and analysis by flow cytometry. (B and C) *In vitro* neutralization by VRC01, 4Dm2m, or LSEVh-LS-F of PBMC infection by HIV-1_{Env}-LucR infectious molecular clones expressing Env from the indicated VRC01-sensitive (B) and VRC01-resistant (C) HIV-1 strains. Activated PBMC from healthy donors were cultured for 48 h in the presence of HIV-1 expressing the indicated Env and the indicated concentration of VRC01, 4Dm2m, or LSEVh-LS-F. Graphed data represent the percent viral neutralization by the indicated concentrations of VRC01, 4Dm2m, and LSEVh-LS-F as measured by luciferase activity and calculated in reference to the untreated infected PBMC using the formula $y = [(1 - \text{treatment RLU})/\text{untreated infected PMBC RLU} \times 100)]$. Each data point in the graph represents the average value of triplicates ± standard deviation (SD). (D) *In vitro* ADCC activity of LSEVh-LS-F. CHO or CHO-gp160SC cells were used as target cells for measuring antibody-mediated effector function as a proxy for ADCC activity of LSEVh-LS-F using as an effector cell a genetically modified Jurkat cell line expressing the human FcRγIIIa with an inducible luciferase reporter gene. Each data point in the graph represents the average value of duplicates ± SD. The control represents no added target cells.

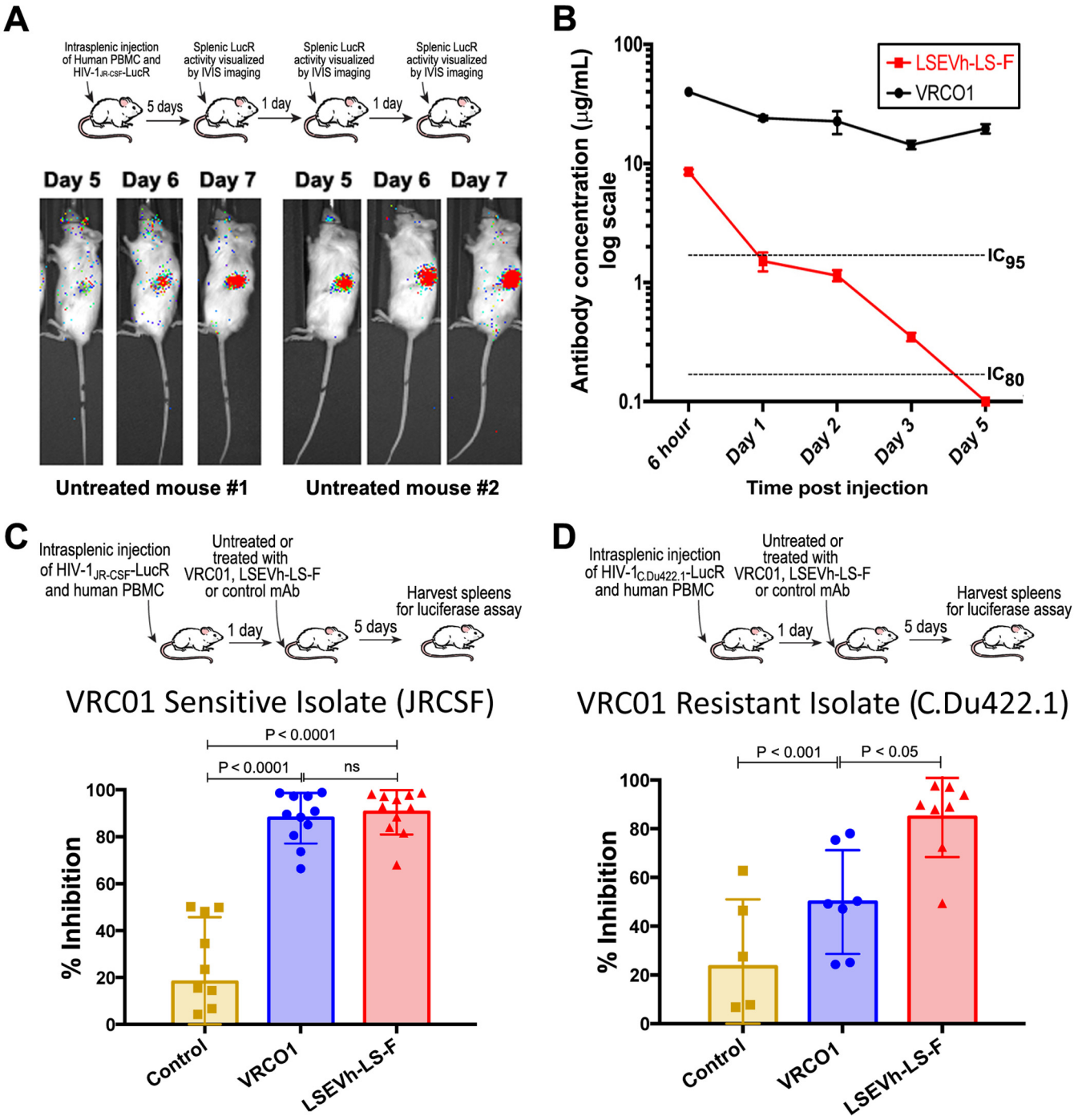

FIG 3 LSEVh-LS-F treatment significantly inhibits *in vivo* infection with VRC01-sensitive and VRC01-resistant HIV-1 isolates. (A) *In vivo* HIV-1_{JRCSF}-LucR infection was visualized using IVIS imaging on days 5, 6, and 7 after viral inoculation. Images were acquired for 3 min after substrate injection and have been corrected for background bioluminescence. Scans of two representative mice are shown. (B) Pharmacokinetics of LSEVh-LS-F and VRC01 *in vivo* in NSG mice. After NSG mice ($n = 2$) were injected with either VRC01 or LSEVh-LS-F, serum was collected 6 h, 1 day, 2 days, 3 days, and 5 days later, and the levels of antibody in each serum sample were determined using a gp140 ELISA. The results are presented on a log scale. The dotted lines on the graph indicate the LSEVh-LS-F levels that neutralize 80% (IC_{80}, 0.17 μg) or at least 95% (IC_{95}, 1.7 μg) of VRC01-sensitive HIV-1 *in vitro*. (C and D) hu-spl-PBMC-NSG mice were inoculated with HIV-1_{Env}-LucR expressing the VRC01-susceptible Env from HIV-1 strain JR-CSF (C) or the VRC01-resistant Env from HIV-1 strain C.Du422.1 (D). The next day, groups of mice were either left untreated or treated with 0.5 mg of either LSEVh-LS-F, VRC01, or control antibody m336. Five days later, HIV-1 infection of the mice was measured by quantifying LucR activity in the splenic lysates. A dot plot graph displays the percent neutralization in each mouse treated with the indicated treatment compared to the untreated group and the group mean ± SD and represent the pooled data from 3 independent experiments using 3 different donors (C) or from 2 independent experiments using 2 different donors (D).

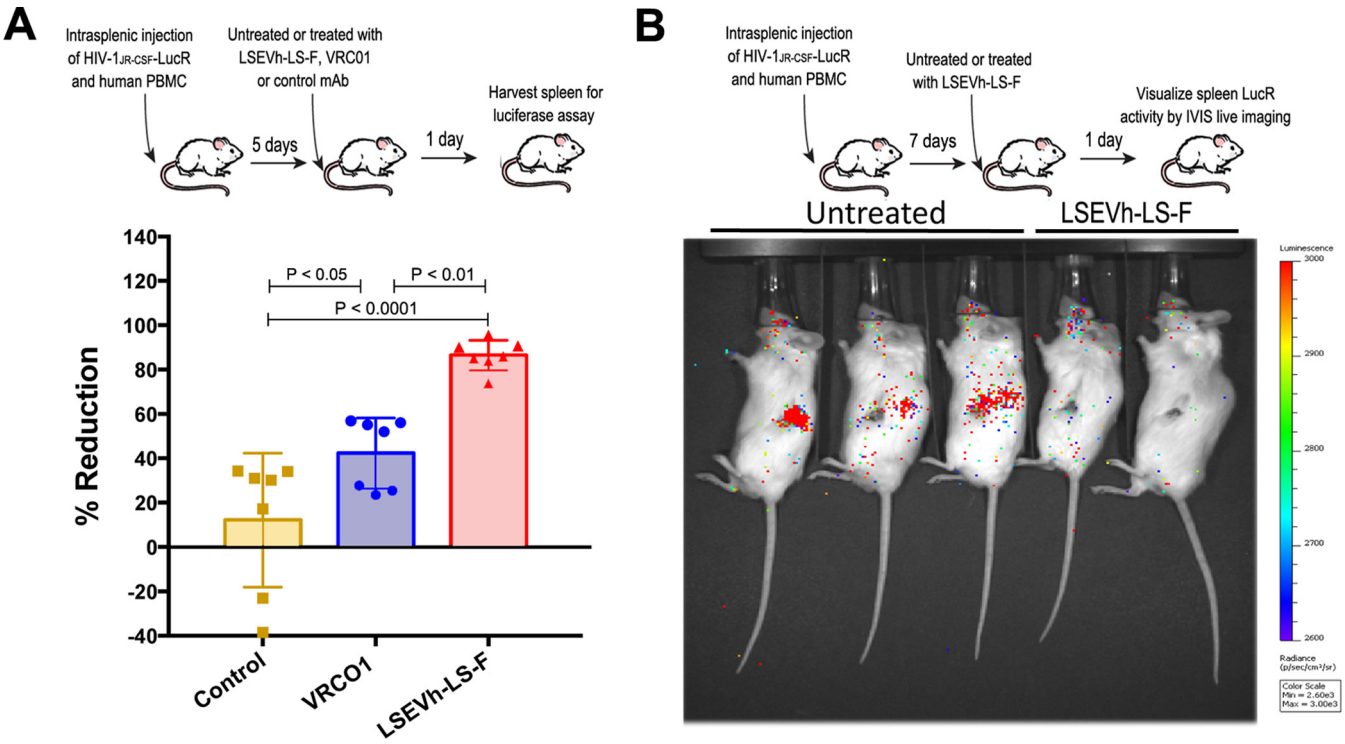

FIG 4 LSEVh-LS-F mobilizes ADCC-mediated *in vivo* elimination of HIV-1-infected cells. (A) Five days after hu-spl-PBMC-NSG mice were inoculated with HIV-1_{JRCSF}-LucR, they were either left untreated or treated with 0.5 mg of LSEVh-LS-F, VRC01, or control antibody m336, and HIV-1 infection was determined by quantifying LucR activity in the splenic lysates the next day. The percent reduction for each mouse compared to the untreated group is presented as a dot plot graph with the group mean ± SD of pooled data from 2 independent experiments using 2 different donors. (B) Seven days after hu-spl-PBMC-NSG mice were inoculated with HIV-1_{JRCSF}-LucR, they were either left untreated or treated with LSEVh-LS-F (0.5 mg). HIV-1 infection indicated by LucR activity was visualized by IVIS live imaging of bioluminescence after injection of the mice with the substrate.

resulted in a highly statistically significant ($P = 0.0001$) reduction of peak viremia at day 9 compared to peak viremia in untreated macaques (Fig. 6C). While at subsequent time points there was a trend of lower virus RNA concentrations in the treated than in the untreated macaques, other than at day 18 ($P = 0.02$), there was no statistically significant decrease in virus RNA (Fig. 6D). These *in vivo* results corresponded with the potent capacity of LSEVh-LS-F to neutralize *in vitro* $SHIV_{SF162P3}$ infection ($IC_{50} = 1.6$ μg/ml, $IC_{80} = 3.9$ μg/ml) (Fig. 6D). To determine whether the transitory inhibitory effect of LSEVh-LS-F on SHIV viremia was due to a short serum half-life, we measured LSEVh-LS-F pharmacokinetics in the infected macaques. The LSEVh-LS-F serum concentration was high (up to 100 μg/ml) at 2 days after infusion but rapidly decreased to <1 μg/ml by 7 days after infusion, a concentration unlikely to be effective in suppressing *in vivo* SHIV replication (Fig. 6E). One month after infection, the macaques were sacrificed, and SHIV infection in the macaque tissues was evaluated for the levels of SHIV RNA. In the ileum, rectum, duodenum, and colon of LSEVh-LS-F-treated macaques, SHIV RNA levels were significantly lower than in the untreated group (Fig. 7A), but the levels of SHIV RNA in the lymph nodes (inguinal, mesenteric, and axillary), brain, and testis/ovary were comparable (Fig. 7B). Thus, while LSEVh-LS-F is highly effective in suppressing *in vivo* SHIV replication, the durability of *in vivo* inhibitory effects of a single dose against SHIV replication was limited by the relatively short serum half-life of LSEVh-LS-F.

DISCUSSION

HIV-1-specific antibodies can eliminate HIV-1-infected cells by ADCC through Fcγ-mediated recruitment of innate immune effector cells, particularly NK cells, which lyse infected cells by exocytosis of granzymes and perforin (30, 31) and may contribute to the prevention and control HIV-1 infection (32, 33). This is supported by studies which

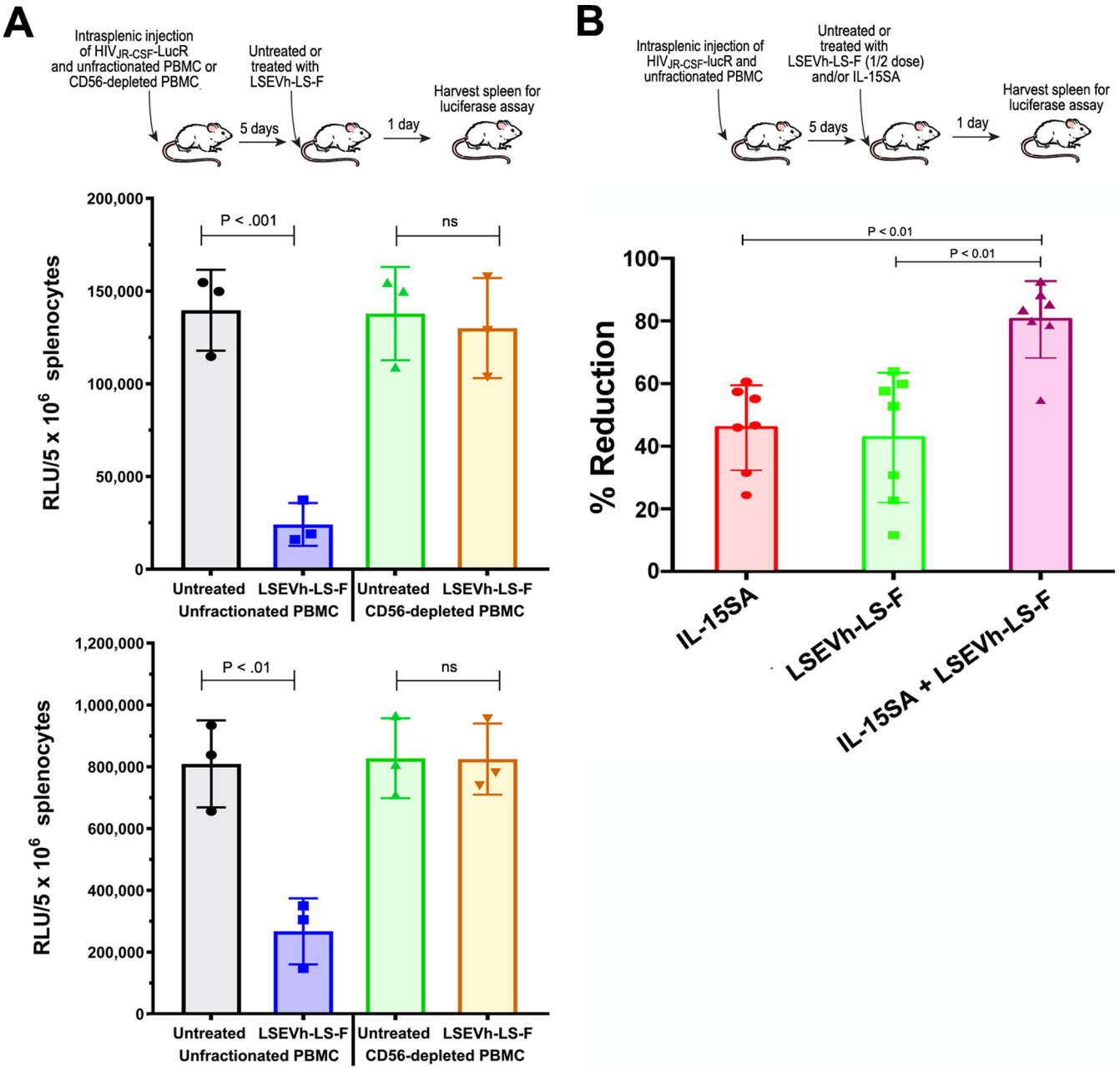

FIG 5 LSEVh-LS-F-induced ADCC requires NK cells for elimination of HIV-1-infected cells. (A) Five days after unfractionated or NK-cell-depleted PBMC were intrasplenically injected into NSG mice (~10^7 cells) together with HIV-1_{JRCSF}-LucR, the mice were left untreated or treated with LSEVh-LS-F (0.5 mg), and 1 day later, LucR activity in the splenic lysates was quantified. Data from two independent experiments are shown as dot plots with the group mean ± SD for each experiment. (B) Five days after hu-spl-PBMC-NSG mice were intrasplenically injected with HIV-1_{JRCSF}-LucR (1×10^7 IU), mice were either left untreated or treated with LSEVh-LS-F (0.25 mg) and/or ALT-803 (0.2 mg/kg), and 1 day later, LucR activity in the splenic lysates was quantified. The percent suppression of infection for each mouse compared to the untreated group is shown as a dot plot with mean ± SD for the group. The graph represents pooled data from 2 independent experiments using one donor.

correlated the magnitude of anti-HIV-1 ADCC activity with the protection of some RV144 HIV-1 vaccine trial subjects (34), slower progression of HIV-1 infection (35, 36), control of infection in elite controllers (37), *in vivo* efficacy of bNAb therapy (31, 38), emergence of immune escape variants (39), and accelerated elimination of HIV-1-infected cells in 3BNC117-treated humanized mice (40). Because ADCC activity correlates with total IgG bound to HIV-1-infected cells (33), the bispecific hexavalent binding of LSEVh-LS-F to the spatially adjacent CD4 and the CD4i coreceptor-binding sites (41) should favor multivalent targeting of individual gp120 trimeric molecules in the HIV-1

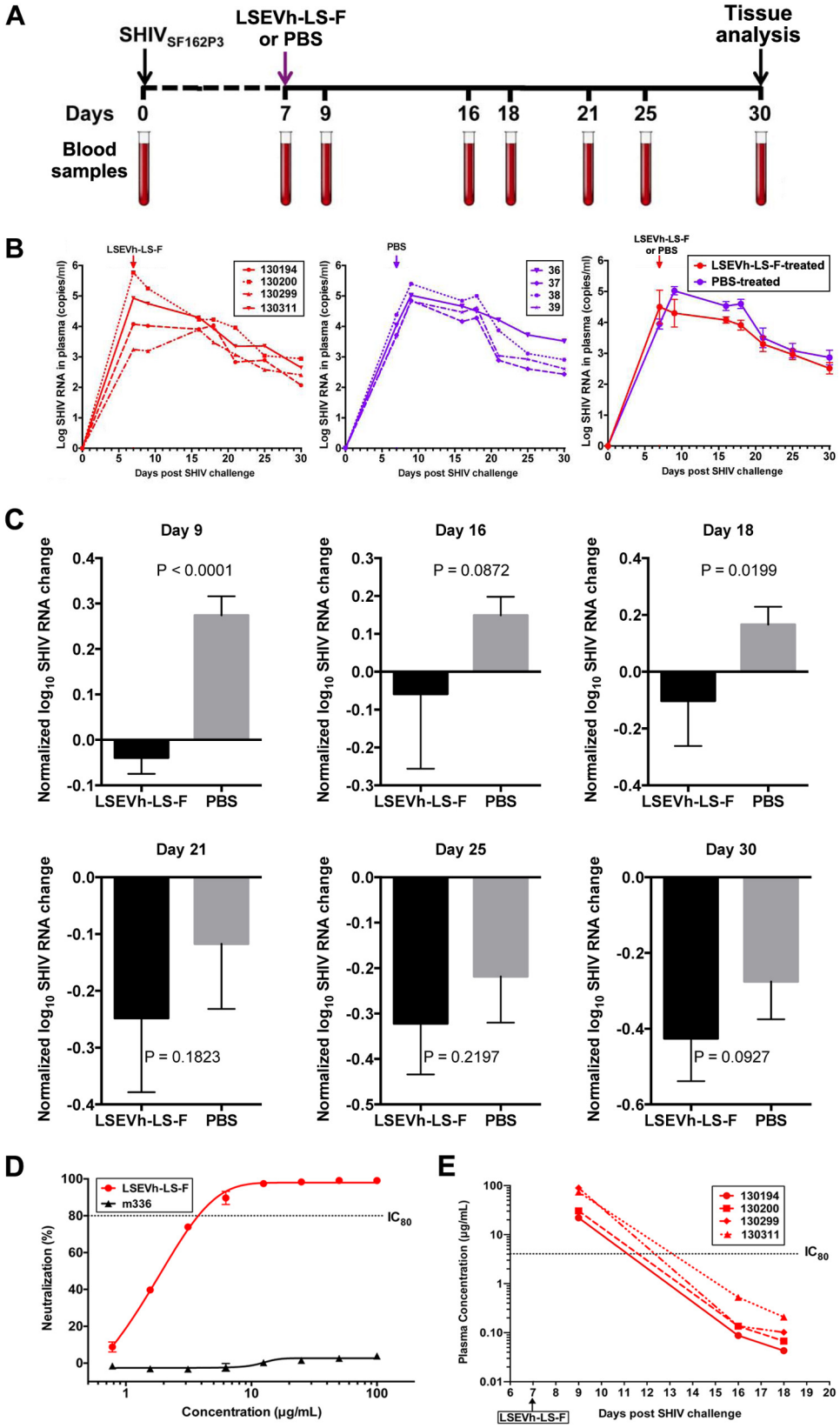

FIG 6 Effect of LSEVh-LS-F treatment on plasma SHIV loads. (A) Experimental treatment and analysis scheme. (B) Eight rhesus macaques were challenged intravenously with SHIV-1$_{SF162P3}$ and treated on day 7 with either a single infusion of LSEVh-LS-F ($n = 4$) or PBS ($n = 4$). Plasma SHIV loads from individual LSEVh-LS-F-treated macaques (left panel) and individual PBS-treated macaques (middle panel) and the average for the four macaques in the

(Continued on next page)

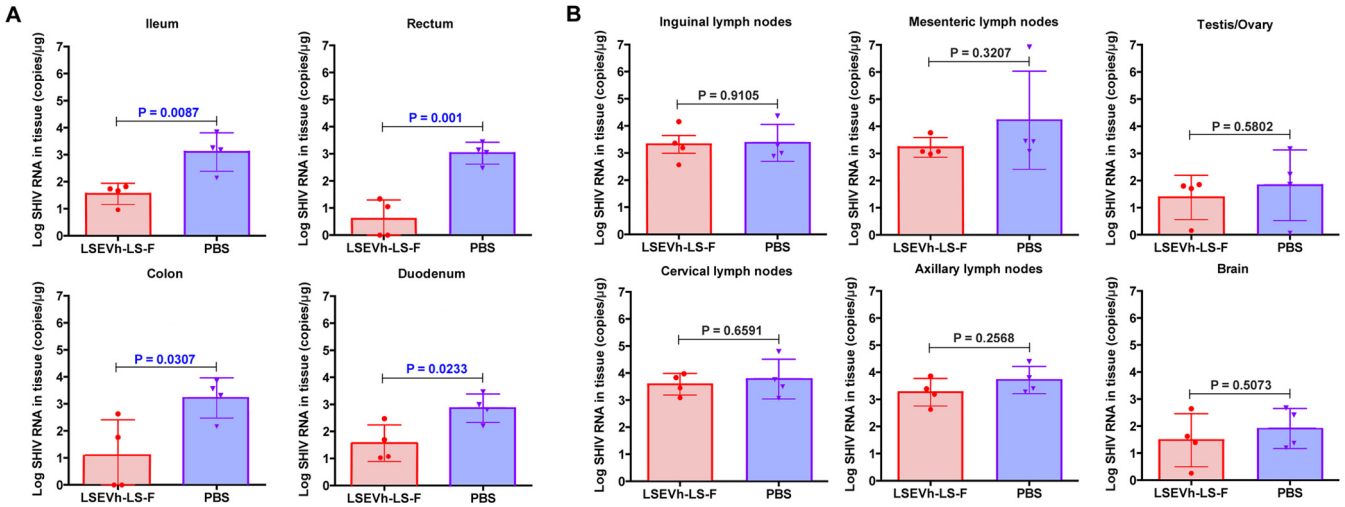

FIG 7 Effect of LSEVh-LS-F treatment on SHIV infection of tissues. Quantification of SHIV RNA in mucosal tissues (A) and lymph nodes, brain, and testes/ovaries (B) is shown. The number of SHIV RNA copies/μg of the indicated tissue in the LSEVh-LS-F-treated and untreated macaques was determined by RT-qPCR at day 30 and is shown for each macaque in a dot plot graph with the mean $\pm$ SD for the group.

membrane, whose wide separation may otherwise prevent efficient bivalent binding by monospecific natural bNAb (42–45), and thereby increase its capacity to mobilize ADCC-mediated elimination of HIV-1-infected cells. Using a strategy reported to enhance the *in vivo* ADCC activity of antibodies used for cancer therapy (17, 18, 46), we defucosylated LSEVh-LS-F to increase the affinity of its Fc domain for FcγRIIIa on innate effector cells and thereby further increase its capacity to mediate HIV-specific ADCC activity. We developed a hu-spl-PBMC-NSG humanized mouse model, which contains human NK cells with high cytotoxic function (26), as an *in vivo* system to evaluate ADCC activity mediated by LSEVh-LS-F. Because full HIV-1 replication in primary T cells takes at least 24 h (27), we postulated that the reduction in the level of HIV-1 infection at 1 day after treatment with LSEVh-LS-F or bNAb should indicate ADCC-mediated *in vivo* elimination of HIV-1-infected cells rather than suppression of new infection by antibody neutralizing activity. The level of HIV-1 infection in hu-spl-PBMC-NSG mice was reduced by $>$80% at 1 day after LSEVh-LS-F treatment, which was 2-fold greater than the reduction mediated by VRC01 treatment (Fig. 4A). These results were confirmed by direct *in vivo* imaging of the LSEVh-LS-F-treated mice by IVIS scanning (Fig. 4B). NK cell depletion abrogated LSEVh-LS-F-mediated reduction in HIV-1 infection, indicating that elimination of HIV-1-infected cells by LSEVh-LS-F was mediated by ADCC (Fig. 5A). This was further supported by our finding that activation of NK cell cytotoxic activity by IL-15SA treatment increased LSEVh-LS-F-mediated *in vivo* reduction in HIV-1 infection (Fig. 5B). In addition to permitting us to determine the *in vivo* ADCC activity of LSEVh-LS-F, the hu-spl-PBMC-NSG humanized mouse model we developed for *in vivo* ADCC evaluation should provide investigators with a crucial high-throughput model to identify HIV-1-specific antibodies, including those with mutated Fc domains (47), and immunomodulators with the most potent *in vivo* capacity to mobilize ADCC activity to eliminate HIV-1-infected cells.

FIG 6 Legend (Continued)

LSEVh-LS-F-treated and PBS-treated groups (right panel) are shown. (C) Analysis with normalized values of the data shown in panel B was performed to decrease the effect of individual macaque variation. Evaluation of the difference in plasma SHIV loads between the treatment and control groups was analyzed by the unpaired *t* test for different days after treatment. The decrease of virus RNA at day 9 for LSEVh-LS-F-treated compared to PBS-treated macaques is highly statistically significant ($P = 0.0001$). (D) Dose-response *in vitro* neutralization of $SHIV_{SF162P3}$ by LSEVh-LS-F assayed in TZM-bl cells. An irrelevant monoclonal antibody, m336, was used as the negative control. (E) Concentration of LSEVh-LS-F after a single infusion of LSEVh-LS-F as a function of time for the individual treated macaques. The limit of detection is about 0.1 μg/ml, and after day 18, the LSEVh-LS-F concentration can be assumed to be undetectable.

In vivo studies in humanized mice, macaques, and humans have demonstrated that treatment with a single bNAb can potently prevent and suppress HIV-1 infection and possibly reduce the HIV-1 latent reservoir by Fc domain-mediated recruitment of effector cells such as by ADCC (6, 7, 9, 47–51). However, a limitation of current bNAb is that no single bNAb neutralizes all strains of HIV-1, enabling the emergence of immune escape variants mutated in bNAb-specific epitopes, likely from preexisting mutant virus (52), and mediating the recurrence of viremia (5, 53). A single amino acid mutation can enable HIV-1 to escape from natural bNAb such as VRC01, 3BNC117, and 10-1074, which is a major impediment currently limiting the efficacy of bNAb monotherapy (7, 54–56). A substantial number of HIV-1-infected individuals are populated with preexisting VRC01-resistant virus, and consequently, treatment of some of these individuals with VRC01 only minimally suppressed viremia (9). VRC01-resistant HIV-1 and 3BNC117-resistant HIV-1 also rapidly emerged during analytical antiretroviral therapy (ART) treatment interruption studies in patients after VRC01 and 3BNC117 administration, respectively (7, 8). Consequently, treatment with combinations of bNAb specific for nonoverlapping epitopes will be required for ADCC-mediated elimination of cells infected with immune escape variants to prevent recurrence of viremia effectuated by resistant virus, emulating the successful strategy of combining different antiretroviral drugs (53). We previously demonstrated that a bispecific Fc domain fusion protein expressing CD4 and the CD4i-gp120 epitope-specific human antibody domain m36 displayed more potent *in vitro* neutralizing activity than Fc domain fusion proteins expressing either CD4 or m36 alone (57). The targeting of two independent gp120 epitopes by LSEVh-LS-F, which contributes to its potent and broad neutralizing activity, should enable it to mediate ADCC elimination while also constraining the *in vivo* emergence of LSEVh-LS-F-resistant HIV-1 escape mutants by requiring mutations in two nonoverlapping gp120 epitopes for immune escape. We demonstrated the *in vivo* inhibitory activity of LSEVh-LS-F against HIV-1 and SHIV by using a humanized mouse model and a nonhuman primate model, respectively. The breadth of LSEVh-LS-F activity was demonstrated by its *in vitro* neutralization of VRC01-resistant Env strains by LSEVh-LS-F (Fig. 2B) and its *in vivo* inhibition of HIV-1 infection by a VRC01-resistant strain, which has also shown resistance to 3BNC117 (Fig. 3D).

An alternate approach to combination therapy with two different bNAb targeting nonoverlapping gp120 epitopes is to generate a bispecific IgG molecule consisting of the antigen-binding fragments from two different bNAb linked to an Fc domain (23, 42). LSEVh-LS-F, which combined a gp120-binding CD4 subunit, mD1.22, and a CD4i coreceptor-binding site-specific antibody fragment, m36.4 (10), differs from bispecific antibodies in three crucial ways. First, instead of using a bNAb domain to recognize the gp120 CD4 binding site, it utilizes a one-domain CD4, mD1.22, that was mutated to exhibit high solubility and stability while retaining binding to all HIV-1 Envs. By mimicking CD4 binding to gp120, mD1.22-resistant escape mutants should display compromised viral replication due to the reduced capacity of their mutated gp120 to bind CD4 and initiate cellular entry and subsequent infection. Second, by engaging with the CD4 binding site of gp120, the mD1.22 induces the exposure of CD4-induced antibody epitopes on gp120, a major target of antibodies circulating in infected patients which mediate ADCC, and boost their capacity to eliminate HIV-1-infected cells via ADCC (20, 58). Third, the bispecific and hexavalent binding of LSEVh-LS-F may increase its avidity for gp120 beyond that of natural monospecific and bivalent antibodies capable of mediating ADCC by facilitating its binding to the limited number of gp120 molecules expressed by HIV-1 and on the surface of HIV-1-infected cells (43). The enhanced avidity of LSEVh-LS-F for gp120 expressed by infected cells was indicated by its increased binding to gp120-expressing ACH2 cells compared to that of VRC01 (Fig. 2A).

Two days after treatment of macaques during acute SHIV infection with LSEVh-LS-F, peak viremia was suppressed by about 1.2 logs compared to that in untreated macaques (Fig. 6B). A similar approach was used to demonstrate that VRC01 alone or the combination of VRC07-523 and PGT121 suppressed acute SHIV infection and reduced

the seeding of cell-associated viral reservoirs, but the experimental protocol for that study differed from ours by sustaining bNAb-mediated viral suppression by initiating ART at 11 days after bNAb treatment (59). The 1.2-log reduction in plasma virus RNA induced by 2 days of LSEVh-LS-F treatment corresponds to $k = 1.38$ day^{-1}, which is higher than the k = 0.36 to 0.89 day^{-1} calculated for macaques chronically infected with SHIV and treated with the bNAb 3BNC117 and 10-1074 (51), indicating that LSEVh-LS-F displays very potent antiretroviral activity. The marked reduction in SHIV infection of LSEVh-LS-F-treated macaque mucosal tissues may be a consequence of the significant reduction in peak viremia mediated by LSEVh-LS-F. This reduction in SHIV-infected mucosal tissues is unlikely to be due to elimination of SHIV-infected cells by LSEVh-LS-F-mediated ADCC, because species differences in the specificity and affinity of the human Fc domain for macaque Fc receptors may limit their capacity to mobilize ADCC in macaques (59, 60). While LSEVh-LS-F plasma levels averaged about 100 μg/ml for the first 2 days after administration, levels subsequently declined more rapidly than those of bNAb such as VRC01 and 3BNC117. As previously described, several factors may contribute to the shorter half-life of LSEVh-LS-F than of native bNAb, including the reduced ability of the CCH1-CK interaction to generate extremely stable heterodimers and the increased susceptibility to proteolytic degradation associated with the use of polypeptide linkers to link mD1.22 and m36.4 to the Fc scaffold (12). We are investigating new approaches to enhance the half-life of LSEVh-LS-F. Nevertheless, its potent capacity to neutralize HIV-1 strains resistant to other bNAb and to eliminate HIV-1-infected cells should counterbalance its shorter half-life, and this supports the potential inclusion of short, intense courses of LSEVh-LS-F as a component of therapeutic regimens that combine immunostimulants, such as ALT-803, and latency-reactivating agents to reduce the HIV-1 reservoir and contribute to the final goal of HIV-1 eradication.

MATERIALS AND METHODS

Cells, viruses, plasmids, proteins, and other reagents. The 293 FreeStyle (293-F) cells were obtained from Invitrogen-Life Technologies (Grand Island, NY). Other cell lines and plasmids used for production of pseudotyped HIV-1 and neutralization assays as well as the SHIV were obtained from the National Institutes of Health AIDS Research and Reference Reagent Program. Generation of HIV-1 infectious molecular clone plasmids is described below. $GP140_{89.6}$ was a gift from Barton F. Haynes (Duke University Medical Center, Durham, NC). Recombinant human FcγRIIIa was purchased from R&D Systems (Minneapolis, MN). Horseradish peroxidase (HRP)-conjugated goat anti-human IgG (Fc-specific) antibody and fluorescein isothiocyanate (FITC)-conjugated goat F(ab′)2 anti-human IgG (γ-specific) antibody were obtained from Sigma-Aldrich (St. Louis, MO).

Expression and purification of VRC01, 4Dm2m, LSEVh-LS, and LSEVh-LS-F. 4Dm2m and LSEVh-LS were produced by transfecting 293-F cells with either the 4Dm2m or LSEVh-LS vector constructed by PCR cloning or the VRC01 plasmid provided by John Mascola (Vaccine Research Center [VRC], NIH, Bethesda, MD) and processing the cell culture supernatant as described previously (10, 12). Defucosylated LSEVh-LS (LSEVh-LS-F) was produced using CHO cells with their GDP-fucose transporter (GFT) genes inactivated using the clustered regularly interspaced short palindromic repeat (CRISPR)/Cas9 system as described previously (19). Briefly, three GDP-fucose transporter gene DNA fragments (target 1, 5′ CGCTGGTCGTCTCTCTCTAC 3′; target 2, 5′ AGATAGGGGTATCCAGCTGC 3′; and target 3, 5′ GTACTTG TTGAGGAATACCA 3′) were cloned into the pCas-Guide-GFP vector (OriGene Technologies, Rockville, MD) and were transfected into CHO cells using Polyfect (Qiagen, Frederick, MD) according to the manufacturer's protocol. Three days after transfection, the green fluorescent protein (GFP)-positive single cells were sorted into 96-well plates and expanded. Successful GDP-fucose transporter gene deletion in one CHO cell knockout mutant clone, CHO-F6, was demonstrated by mass spectral analysis of purified antibodies obtained after transient antibody expression. CHO-F6 was adapted for growth in serum-free medium and was transfected with the LSEVh-LS vector to establish stable cell lines producing LSEVh-LS-F using the standard glutamine synthetase-based selection system (61). 4Dm2m, LSEVh-LS, and LSEVh-LS-F were purified from the 293-F and CHO-F6 cell culture supernatants by protein A-Sepharose 4 Fast Flow column chromatography (GE Healthcare, Piscataway Township, NJ) as described previously (11).

High-resolution MS. The proteins were mixed with buffer (7.5 M guanidine-HCl, 0.1 M Tris-HCl, and 1 mM EDTA) in the presence of 20 mM dithiothreitol (DTT) and incubated at 70°C for 15 min. Mass spectrometry (MS) data were acquired on an Agilent 6520 Accurate-Mass Q-TOF LC/MS system (Agilent Technologies, Danbury, CT) equipped with a dual electrospray source, operated in the positive-ion mode. Separation was performed on a Zorbax 300SB-C3 Poroshell column (2.1 mm by 75 mm; particle size, 5 μm). The analytes were eluted at a flow rate of 1 ml/min with a 1 to 90% organic gradient over 5 min and holding organic for 1 min. Both mobile phases, water and acetonitrile, contained 0.1% formic acid. The instrument was used in a full-scan time-of-flight (TOF) mode. MS source parameters were set with

a capillary voltage of 4 kV, fragmentor voltage of 220 V, and skimmer voltage of 65 V. The gas temperature was 350°C, the drying gas flow 12 liters/min, and nebulizer pressure 55 lb/in^2 gauge. Data were acquired at high resolution (3,200 *m/z*) and 4 GHz. TOF-mass spectra were recorded across the range of 100 to 3,200 *m/z*. Mass accuracy was maintained during the run time by infusing an internal mass calibration sample continuously during the liquid chromatography (LC)-MS runs. Data acquisition was performed using a Mass Hunter work station (Agilent, version B.02.00), and data analysis and deconvolution of mass spectra were performed using Mass Hunter qualitative analysis software (Agilent, version B.03.01) with BioConfirm Workflow.

SPR. The kinetics and affinity of LSEVh-LS and LSEVh-LS-F binding to FcγRIIIa were quantified by surface plasmon resonance (SPR) analysis on a Biacore X100 instrument (GE Healthcare, Port Washington, NY) using a single-cycle approach according to the manufacturer's instructions. Briefly, purified proteins were diluted in sodium acetate (pH 5.0) and immobilized directly onto a CM5 sensor chip with the standard amine coupling method. The reference cell was injected with *N*-hydroxysuccinimide–1-ethyl-3-(3-dimethyaminopropy)carbodiimide and ethanolamine without injection of FcγRIIIa. Analytes were tested at 1,000, 500, 250, 125, and 62.5 nM concentrations. Kinetic constants were calculated from the sensograms fitted with the monovalent binding model of the BiacoreX100 evaluation software 2.0.

Generation of HIV-1 infectious molecular clones. Inhibition of *in vitro* and *in vivo* HIV-1 infection was determined utilizing the LucR reporter-expressing HIV-1 infectious molecular clone (IMC) system (62), in which the proviral genome has been engineered to express, in *cis*, the LucR reporter gene and heterologous HIV-1 *env* gene sequences of choice. The approach is well established in multiple contexts, including the evaluation of the *in vitro* and *in vivo* HIV-1 inhibitory capacities of antibodies, NK cells, CD8$^+$ T cells, dual-affinity retargeting proteins (DARTs), and microbicides (26, 63). Proviral plasmids, collectively referred to as pNL-LucR.T2A-Env.ecto (62), carrying the *env* genes indicated below were transiently transfected into 293T cells to produce virus stocks of HIV-1 IMC expressing LucR (HIV-1$_{Env}$-LucR). HIV-1$_{Env}$-LucR reporter viruses are replication competent and continue to express LucR over multiple cycles of replication, which permits the highly sensitive and specific detection of active HIV-1 replication for several weeks after inoculation (62). Because LucR has a short cellular half-life of approximately 3 h (64), the measurement of LucR levels correlates with active HIV-1 replication. For these experiments we used HIV-1$_{Env}$-LucR viruses with VRC01-sensitive HIV-1 Env strains JR-CSF, Bal, and 45_01dH5 (clade B) and C.1176 (clade C) and resistant Env strains 45_01E11 (clade B) and C.Du151.2, C.Du172.17, and C.Du422.1 (clade C) (21, 22). HIV-1 Env C.Du422.1is also resistant to neutralization by the bNAb 3BNC117 (23, 24). The infectious titer of HIV-1$_{Env}$-LucR viruses (on average 5×10^6 to 10×10^6 infectious units [IU]/ml) was determined by a limiting-dilution infection assay using TZM-bl cells as described previously (62).

Assay of antibody binding to cell surface Env. Binding of LSEVh-LS-F to Env trimers expressed on the surface of infected cells and comparison to VRC01 binding was performed by flow cytometric analysis. LSEVh-LS-F, VRC01, and a control MAb recognizing Ebola virus, ADI-15878, were biotinylated using EZ-Link sulfo-NHS-LC-biotin (Life Technologies) followed by a desalting step using a Zeba spin desalting column (Life Technologies). ACH-2 cells, a latently infected T cell line used as a model of HIV-1 latency (20), were activated with phorbol myristate acetate (PMA) (2 ng/ml) for 48 h and then stained with each biotinylated antibody at the indicated concentration determined after biotinylation for 30 min at 4°C, followed by washing and incubation with streptavidin-phycoerythrin (PE) (Life Technologies) at a 1:1,000 dilution for 30 min at 4°C. Data were acquired using an LSR II flow cytometer (BD Biosciences) and analyzed with FlowJo software (FlowJo, Ashland, OR).

***In vitro* neutralization assays in human PBMC.** The capacity of VRC01, 4Dm2m, and LSEVh-LS-F to neutralize HIV-1$_{Env}$-LucR expressing HIV-1 envelopes from VRC01-susceptible (HIV-1$_{Bal}$-LucR, HIV-1$_{JR\text{-}CSF}$-LucR, HIV-1$_{C.1176}$-LucR, and HIV-1$_{45_01dH5}$-LucR) and VRC01-resistant (HIV-1$_{Du151.2}$-LucR, HIV-1$_{Du172.17}$-LucR, HIV-1$_{Du422.1}$-LucR, and HIV-1$_{45_01E11}$-LucR) viruses (21, 22) was determined using a modified *in vitro* human PBMC-based assay described previously (62). Human PBMC were isolated from HIV-1 naive donors, activated with phytohemagglutinin (PHA) (4 μg/ml) and IL-2 (100 U/ml), and cultured at 37°C in R-10 (RPMI 1640 with added heat-inactivated fetal bovine serum [FBS] [10%, vol/vol], penicillin [100 U/ml], streptomycin [10 μg/ml], glutamine [2 mM], and HEPES [10 mM]). One day later, the HIV-1$_{Env}$-LucR viruses (6.25×10^4 IU) were coincubated for 1 h at 37°C in a 96-well round-bottom plate with 10-fold dilutions (0.01 nM to 100 nM) of either 4Dm2m, LSEVh-LS-F, or VRC01. The activated PBMC were harvested, washed, resuspended in R10 medium, added to each well (1×10^5 cells/well) with the antibody-virus mixtures, and placed in culture. After 48 h, the supernatant was aspirated, the cells were lysed with LucR assay lysis buffer (100 μl/well), and the LucR activity in an aliquot (20 μl) of each lysate was measured using the *Renilla* luciferase assay system (Promega, Madison, WI) as described previously (26).

***In vitro* ADCC assay.** As target cells, CHO cells or CHO cells which stably express a clade-B HIV-1 Env (CHO-gp160SC cells) suspended in R10 were plated (2.5×10^4 cells/well) into 96-well plates (25 μl/well), and the indicated concentration of LSEVh-LS-F diluted in R10 was added to each well (50 μl/well). For effector cells, genetically modified Jurkat cells expressing the human FcγRIIIa with a luciferase reporter gene under the transcriptional control of the NFAT-RE (Promega) were added (1.5×10^5 cells/well in 25 μl R10) for a target/effector cell ratio of 1:6. After overnight incubation at 37°C, the Bio-Glo Luciferase assay reagent (Promega) was added, and luminescence quantified as relative luminescence units (RLU) was measured using a luminescence plate reader.

Pharmacokinetic measurement of serum levels of VRC01 and LSEVh-LS-F in mice and in rhesus macaques. NSG mice were intravenously injected with 0.5 mg of either VRC01 or LSEVh-LS-F on day 0. Plasma samples were collected by submandibular bleeding at the indicated times after injection.

Chinese-origin rhesus macaques were intravenously injected with LSEVh-LS-F (10 mg/kg) at day 7 after SHIV infection, and plasma samples were collected at days 0, 7, 9, 16, 18, 21, 25, and 30. Plasma concentrations of VRC01 and LSEVh-LS-F were determined by enzyme-linked immunosorbent assay (ELISA) with plates coated with HIV-1 Env $gp140_{89.6.}$ Standard curves were generated using VRC01 or LSEVh-LS-F standards as described previously (12).

Measurement of the *in vivo* capacity of LSEVh-LS-F to inhibit HIV-1 infection. The *in vivo* capacity of LSEVh-LS-F or VRC01 to inhibit HIV-1 infection was determined using our previously described humanized mouse model, in which NOD-SCID-IL-2r$\gamma^{-/-}$ (NSG) mice were intrasplenically injected with activated human PBMC (hu-spl-PBMC-NSG mice) (26). Briefly, human PBMC isolated from HIV-1-naive donors were cultured in R10 and activated with PHA (4 μg/ml) and IL-2 (100 U/ml) for 24 h at 37°C. In some experiments, NK cells were removed from the PBMC after activation by immunomagnetic sorting using anti-human CD56 microbeads (Miltenyi Biotec, Cambridge, MA). Depletion (>95%) was confirmed by flow cytometric analysis after staining with anti-human CD3-FITC and anti-human CD56-PE (BioLegend) antibodies as described previously (26). The next day, after the activated PBMC or NK cell-depleted PBMC were washed twice with sterile PBS, HIV-1-LucR was added ($\sim 1 \times 10^6$ IU/10^7 PBMC) to the activated PBMC, and the cells were centrifuged for 1 h at 25°C at 2,500 rpm, resuspended, and injected intrasplenically ($\sim 10^7$ cells/mouse) into NSG mice (Jackson Laboratories, Bar Harbor, ME). The mice were bred and maintained in our biosafety level 2 (BSL2)-enhanced animal facility at Albert Einstein College of Medicine as described previously (65). The capacity of LSEVh-LS-F or VRC01 to inhibit HIV-1 infection was evaluated by intravenously injecting hu-spl-PBMC-NSG mice with VRC01 (0.5 mg) or LSEVh-LS-F (0.5 mg) at 1 day after intrasplenic inoculation with the indicated HIV-1_{Env}-LucR. As a negative control, we used m336, a monoclonal antibody against the Middle East respiratory syndrome coronavirus (66). The level of HIV-1 infection in the engrafted human PBMC in hu-spl-PBMC-NSG mouse spleens was quantified by measuring the LucR activity in the mouse splenic lysates using the *Renilla* luciferase assay system (Promega), as previously described (26). To enable us to combine the results of multiple experiments for statistical analysis, the results are reported as percent neutralization of HIV-1 infection by each treatment group in reference to the untreated group using the formula $y = [(1 - \text{treated group RLU})/\text{untreated group RLU} \times 100]$.

To determine the *in vivo* capacity of LSEVh-LS-F or VRC01 to eliminate HIV-1-infected cells, hu-spl-PBMC-NSG mice or NSG mice intrasplenically injected with NK cell-depleted PBMC ($\sim 10^7$ cells/mouse) were intravenously injected with either LSEVh-LS-F (0.5 mg) or VRC01 (0.5 mg) at 5 days after infection with the indicated HIV-1_{Env}-LucR, to provide time for the establishment of *in vivo* infection and sufficient HIV-1-infected targets to evaluate the effectiveness of ADCC-mediated elimination of HIV-1-infected cells. For some experiments, the mice were intravenously injected with LSEVh-LS-F (0.25 mg) and/or subcutaneously injected with a dose of the IL-15SA ALT-803 (0.2 mg/kg), which provides the mice with a maximum concentration in serum (C_{max}) of ~25 nM (26). The day after treatment, the reduction in the number of HIV-1-infected cells in the mouse spleens was determined by quantifying the decrease in LucR activity compared to LucR levels in the untreated group using the formula $y = [(1 - \text{treated group RLU})/\text{untreated group RLU} \times 100]$.

IVIS imaging. *In vivo* HIV-1 infection in the hu-spl-PBMC mice was visualized and quantified by bioluminescent imaging using the IVIS Spectrum imager (Caliper LifeSciences, Hopkinton, MA) after the mice were intravenously injected (5 μg/mouse) with the bioluminescence substrate RediJect Coelenterazine h (Caliper Life Sciences). The images were analyzed using the Wizard bioluminescent selection tool for automatic wavelength and exposure detection, and the bioluminescent and gray-scale images were overlaid using the LivingImage 4.0 software package to create a pseudocolor image that represents bioluminescence intensity. The bioluminescent intensity of the luciferase activity in the mouse spleens was quantified using the LivingImage 4.0 software package and reported as photon counts/second.

Measurement of LSEVh-LS-F inhibitory activity in SHIV-infected macaques. Eight healthy male and female Chinese-origin rhesus macaques were randomly assigned to two groups (four in each), injected intravenously with $SHIV_{SF162P3}$ (1,000 50% tissue culture infective doses [$TCID_{50}$]), and 7 days later intravenously injected with LSEVh-LS or PBS. Whole blood was collected at days 0, 7, 9, 16, 18, 21, 25, and 30. All animals were sacrificed at day 30, and tissue samples were collected and stored at −80°C. *In vitro* neutralization of $SHIV_{SF162P3}$ by LSEVh-LS-F was evaluated using the TZM-bl assay (67). Briefly, serially diluted LSEVh-LS-F and the irrelevant control antibody m336 were preincubated with $SHIV_{SF162P3}$ for 1 h at 37°C before being added to the TZM-bl cells in a 96-well plate. The luciferase expression was quantified 48 h after infection upon cell lysis and the addition of luciferase substrate (Invitrogen).

To precisely measure the viral RNA from plasma and necropsy tissues, we utilized a new ultrasensitive, nested, quantitative real-time PCR (RT-qPCR) method targeting a highly conserved region in simian immunodeficiency virus (SIV) gag (68). SIV/SHIV RNA loads in plasma and tissues were quantified by extracting RNA either from plasma (500 μl) using the QIAamp viral RNA minikit (Qiagen) or from tissues (~100 mg) pulverized with stainless steel grinding balls and homogenized in TRIzol reagent following the manufacturer's recommendations. We used "nested" primers SIVnestF01 (GATTTGGATTAGCAGAAA GCCTGTTG) and SIVnestR01 (GTTGGTCTACTTGTTTTTGGCATAGTTTC) flanking the SIV gag target region for reverse transcription and preamplification. The RNA was reverse transcribed into cDNA using the nested primer SIVnestR01 to facilitate priming of specific target sequences, avoid generation of nonspecific sequences, and further enhance the sensitivity of detection. The cDNA was then preamplified by PCR for 12 cycles (94°C for 30s, 60°C for 1 min, and 72°C for 1 min) with the nested primers and amplified by real-time quantitative PCR for SIV DNA gag for 45 cycles (95°C for 10 s and 60°C for 1 min) using the forward primer SGAG21 (5′-GTCTGCGTCATPTGGTGCATTC-3′) and the reverse primer SGAG22 (5′-CACT AGKTGTCTCTGCACTATPTGTTTTG-3′). The amplified product was detected by hybridization to the la-

beled probe pSGAG23 (5′-FAM-CTTCPTCAGTKTGTTTCACTTTCTCTTCTGCG-BHQ1-3′). Quantitative determinations for samples showing amplification in all replicates were derived directly with reference to a linearized SIVmac239 standard curve (triplicate reactions for 10 dilutions from 10^1 copies/reaction to 10^7 copies/reaction) by averaging the values determined for each reaction based on interpolation of the measured threshold cycle values onto the standard curve of input template copy number versus threshold cycle values performed with each assay.

Statistical analysis. The statistical significance of the *in vivo* neutralization or suppression of HIV-1 infection by the different treatment groups compared to the untreated group was determined through the one-way analysis of variance (ANOVA) multiple-comparison test or the unpaired *t* test. GraphPad Prism software was used for the statistical analysis, and differences were considered statistically significant when the *P* value was <0.05.

Study approval. All the mouse studies were approved by the Institute for Animal Studies and the Institutional Review Board at Albert Einstein College of Medicine in compliance with the human and animal experimentation guidelines of the U.S. Department of Health and Human Services and adherence to the NIH Guide for the Care and Use of Laboratory Animals. The macaque studies were conducted in the biosafety level 3 laboratory with protocols approved by the Institutional Animal Care and Use Committee of the Institute of Laboratory Animal Science, Chinese Academy of Medical Sciences.

ACKNOWLEDGMENTS

This work was supported by the National Institute of Drug Abuse at the National Institutes of Health (DA033788 and DA036171 to H.G.), the National Institute of Allergy and Infectious Diseases at the National Institutes of Health (UM1AI26617 to H.G), the Einstein-Rockefeller-CUNY Center for AIDS Research (P30-AI124414) (which is supported by the following NIH cofunding and participating institutes and centers: NIAID, NCI, NICHD, NHBL, NIDA, NIMH, NIA, FIC, and OAR and the intramural research program of the NCI, National Institutes of Health, Department of Health and Human Services [DHHS]), the Charles Michael Chair in Autoimmune Diseases (to H.G.), U.S.-China Program for Research Toward a Cure for HIV-1/AIDS, the National Natural Science Foundation of China (31570936 and 81561128006), and the Shanghai Pujiang Talent Program (15PJ1400800).

We thank Yanping Wang for help with the production of LSEVh-LS-F.

H. Wong and E. Jeng are employees and stockholders of Altor BioScience Corporation, which provided the IL-15 superagonist ALT-803.

The content of this publication does not necessarily reflect the views or policies of the DHHS, nor does mention of trade names, commercial products, or organizations imply endorsement by the US government.

REFERENCES

1. Walker LM, Huber M, Doores KJ, Falkowska E, Pejchal R, Julien JP, Wang SK, Ramos A, Chan-Hui PY, Moyle M, Mitcham JL, Hammond PW, Olsen OA, Phung P, Fling S, Wong CH, Phogat S, Wrin T, Simek MD, Koff WC, Wilson IA, Burton DR, Poignard P. 2011. Broad neutralization coverage of HIV by multiple highly potent antibodies. Nature 477:466–470. https://doi.org/10.1038/nature10373.
2. Euler Z, Alter G. 2015. Exploring the potential of monoclonal antibody therapeutics for HIV-1 eradication. AIDS Res Hum Retroviruses 31:13–24. https://doi.org/10.1089/aid.2014.0235.
3. Lee WS, Parsons MS, Kent SJ, Lichtfuss M. 2015. Can HIV-1-specific ADCC assist the clearance of reactivated latently infected cells? Front Immunol 6:265. https://doi.org/10.3389/fimmu.2015.00265.
4. Bruel T, Guivel-Benhassine F, Amraoui S, Malbec M, Richard L, Bourdic K, Donahue DA, Lorin V, Casartelli N, Noel N, Lambotte O, Mouquet H, Schwartz O. 2016. Elimination of HIV-1-infected cells by broadly neutralizing antibodies. Nat Commun 7:10844. https://doi.org/10.1038/ncomms10844.
5. Horwitz JA, Halper-Stromberg A, Mouquet H, Gitlin AD, Tretiakova A, Eisenreich TR, Malbec M, Gravemann S, Billerbeck E, Dorner M, Buning H, Schwartz O, Knops E, Kaiser R, Seaman MS, Wilson JM, Rice CM, Ploss A, Bjorkman PJ, Klein F, Nussenzweig MC. 2013. HIV-1 suppression and durable control by combining single broadly neutralizing antibodies and antiretroviral drugs in humanized mice. Proc Natl Acad Sci U S A 110:16538–16543. https://doi.org/10.1073/pnas.1315295110.
6. Caskey M, Klein F, Lorenzi JC, Seaman MS, West AP, Jr, Buckley N, Kremer G, Nogueira L, Braunschweig M, Scheid JF, Horwitz JA, Shimeliovich I, Ben-Avraham S, Witmer-Pack M, Platten M, Lehmann C, Burke LA, Hawthorne T, Gorelick RJ, Walker BD, Keler T, Gulick RM, Fatkenheuer G, Schlesinger SJ, Nussenzweig MC. 2015. Viraemia suppressed in HIV-1-infected humans by broadly neutralizing antibody 3BNC117. Nature 522:487–491. https://doi.org/10.1038/nature14411.
7. Scheid JF, Horwitz JA, Bar-On Y, Kreider EF, Lu CL, Lorenzi JC, Feldmann A, Braunschweig M, Nogueira L, Oliveira T, Shimeliovich I, Patel R, Burke L, Cohen YZ, Hadrigan S, Settler A, Witmer-Pack M, West AP, Jr, Juelg B, Keler T, Hawthorne T, Zingman B, Gulick RM, Pfeifer N, Learn GH, Seaman MS, Bjorkman PJ, Klein F, Schlesinger SJ, Walker BD, Hahn BH, Nussenzweig MC, Caskey M. 2016. HIV-1 antibody 3BNC117 suppresses viral rebound in humans during treatment interruption. Nature 535:556–560. https://doi.org/10.1038/nature18929.
8. Bar KJ, Sneller MC, Harrison LJ, Justement JS, Overton ET, Petrone ME, Salantes DB, Seamon CA, Scheinfeld B, Kwan RW, Learn GH, Proschan MA, Kreider EF, Blazkova J, Bardsley M, Refsland EW, Messer M, Clarridge KE, Tustin NB, Madden PJ, Oden K, O'Dell SJ, Jarocki B, Shiakolas AR, Tressler RL, Doria-Rose NA, Bailer RT, Ledgerwood JE, Capparelli EV, Lynch RM, Graham BS, Moir S, Koup RA, Mascola JR, Hoxie JA, Fauci AS, Tebas P, Chun T-W. 2016. Effect of HIV antibody VRC01 on viral rebound after treatment interruption. N Engl J Med 375:2037–2050. https://doi.org/10.1056/NEJMoa1608243.
9. Lynch RM, Boritz E, Coates EE, DeZure A, Madden P, Costner P, Enama ME, Plummer S, Holman L, Hendel CS, Gordon I, Casazza J, Conan-Cibotti M, Migueles SA, Tressler R, Bailer RT, McDermott A, Narpala S, O'Dell S, Wolf G, Lifson JD, Freemire BA, Gorelick RJ, Pandey JP, Mohan S, Chomont N, Fromentin R, Chun TW, Fauci AS, Schwartz RM, Koup RA, Douek DC, Hu Z, Capparelli E, Graham BS, Mascola JR, Ledgerwood JE.

2015. Virologic effects of broadly neutralizing antibody VRC01 administration during chronic HIV-1 infection. Sci Transl Med 7:319ra206. https://doi.org/10.1126/scitranslmed.aad5752.
10. Chen W, Feng Y, Prabakaran P, Ying T, Wang Y, Sun J, Macedo CD, Zhu Z, He Y, Polonis VR, Dimitrov DS. 2014. Exceptionally potent and broadly cross-reactive, bispecific multivalent HIV-1 inhibitors based on single human CD4 and antibody domains. J Virol 88:1125–1139. https://doi.org/10.1128/JVI.02566-13.
11. Chen W, Zhu Z, Feng Y, Dimitrov DS. 2008. Human domain antibodies to conserved sterically restricted regions on gp120 as exceptionally potent cross-reactive HIV-1 neutralizers. Proc Natl Acad Sci U S A 105:17121–17126. https://doi.org/10.1073/pnas.0805297105.
12. Chen W, Bardhi A, Feng Y, Wang Y, Qi Q, Li W, Zhu Z, Dyba MA, Ying T, Jiang S, Goldstein H, Dimitrov DS. 2016. Improving the CH1-CK heterodimerization and pharmacokinetics of 4Dm2m, a novel potent CD4-antibody fusion protein against HIV-1. MAbs 8:761–774. https://doi.org/10.1080/19420862.2016.1160180.
13. Moldt B, Shibata-Koyama M, Rakasz EG, Schultz N, Kanda Y, Dunlop DC, Finstad SL, Jin C, Landucci G, Alpert MD, Dugast AS, Parren PW, Nimmerjahn F, Evans DT, Alter G, Forthal DN, Schmitz JE, Iida S, Poignard P, Watkins DI, Hessell AJ, Burton DR. 2012. A nonfucosylated variant of the anti-HIV-1 monoclonal antibody b12 has enhanced FcgammaRIIIa-mediated antiviral activity in vitro but does not improve protection against mucosal SHIV challenge in macaques. J Virol 86:6189–6196. https://doi.org/10.1128/JVI.00491-12.
14. Shinkawa T, Nakamura K, Yamane N, Shoji-Hosaka E, Kanda Y, Sakurada M, Uchida K, Anazawa H, Satoh M, Yamasaki M, Hanai N, Shitara K. 2003. The absence of fucose but not the presence of galactose or bisecting N-acetylglucosamine of human IgG1 complex-type oligosaccharides shows the critical role of enhancing antibody-dependent cellular cytotoxicity. J Biol Chem 278:3466–3473. https://doi.org/10.1074/jbc.M210665200.
15. Shields RL, Lai J, Keck R, O'Connell LY, Hong K, Meng YG, Weikert SH, Presta LG. 2002. Lack of fucose on human IgG1 N-linked oligosaccharide improves binding to human Fcgamma RIII and antibody-dependent cellular toxicity. J Biol Chem 277:26733–26740. https://doi.org/10.1074/jbc.M202069200.
16. Gagez AL, Cartron G. 2014. Obinutuzumab: a new class of anti-CD20 monoclonal antibody. Curr Opin Oncol 26:484–491. https://doi.org/10.1097/CCO.0000000000000107.
17. Suzuki E, Niwa R, Saji S, Muta M, Hirose M, Iida S, Shiotsu Y, Satoh M, Shitara K, Kondo M, Toi M. 2007. A nonfucosylated anti-HER2 antibody augments antibody-dependent cellular cytotoxicity in breast cancer patients. Clin Cancer Res 13:1875–1882. https://doi.org/10.1158/1078-0432.CCR-06-1335.
18. Junttila TT, Parsons K, Olsson C, Lu Y, Xin Y, Theriault J, Crocker L, Pabonan O, Baginski T, Meng G, Totpal K, Kelley RF, Sliwkowski MX. 2010. Superior in vivo efficacy of afucosylated trastuzumab in the treatment of HER2-amplified breast cancer. Cancer Res 70:4481–4489. https://doi.org/10.1158/0008-5472.CAN-09-3704.
19. Chan KF, Shahreel W, Wan C, Teo G, Hayati N, Tay SJ, Tong WH, Yang Y, Rudd PM, Zhang P, Song Z. 2016. Inactivation of GDP-fucose transporter gene (Slc35c1) in CHO cells by ZFNs, TALENs and CRISPR-Cas9 for production of fucose-free antibodies. Biotechnol J 11:399–414. https://doi.org/10.1002/biot.201500331.
20. Lee WS, Richard J, Lichtfuss M, Smith AB 3rd, Park J, Courter JR, Melillo BN, Sodroski JG, Kaufmann DE, Finzi A, Parsons MS, Kent SJ. 2015. Antibody-dependent cellular cytotoxicity against reactivated HIV-1-infected cells. J Virol 90:2021–2030. https://doi.org/10.1128/JVI.02717-15.
21. Wu X, Wang C, O'Dell S, Li Y, Keele BF, Yang Z, Imamichi H, Doria-Rose N, Hoxie JA, Connors M, Shaw GM, Wyatt RT, Mascola JR. 2012. Selection pressure on HIV-1 envelope by broadly neutralizing antibodies to the conserved CD4-binding site. J Virol 86:5844–5856. https://doi.org/10.1128/JVI.07139-11.
22. Wu X, Yang ZY, Li Y, Hogerkorp CM, Schief WR, Seaman MS, Zhou T, Schmidt SD, Wu L, Xu L, Longo NS, McKee K, O'Dell S, Louder MK, Wycuff DL, Feng Y, Nason M, Doria-Rose N, Connors M, Kwong PD, Roederer M, Wyatt RT, Nabel GJ, Mascola JR. 2010. Rational design of envelope identifies broadly neutralizing human monoclonal antibodies to HIV-1. Science 329:856–861. https://doi.org/10.1126/science.1187659.
23. Bournazos S, Gazumyan A, Seaman MS, Nussenzweig MC, Ravetch JV. 2016. Bispecific anti-HIV-1 antibodies with enhanced breadth and potency. Cell 165:1609–1620. https://doi.org/10.1016/j.cell.2016.04.050.
24. Scheid JF, Mouquet H, Ueberheide B, Diskin R, Klein F, Oliveira TY, Pietzsch J, Fenyo D, Abadir A, Velinzon K, Hurley A, Myung S, Boulad F, Poignard P, Burton DR, Pereyra F, Ho DD, Walker BD, Seaman MS, Bjorkman PJ, Chait BT, Nussenzweig MC. 2011. Sequence and structural convergence of broad and potent HIV antibodies that mimic CD4 binding. Science 333:1633–1637. https://doi.org/10.1126/science.1207227.
25. Cheng ZJ, Garvin D, Paguio A, Moravec R, Engel L, Fan F, Surowy T. 2014. Development of a robust reporter-based ADCC assay with frozen, thaw-and-use cells to measure Fc effector function of therapeutic antibodies. J Immunol Methods 414:69–81. https://doi.org/10.1016/j.jim.2014.07.010.
26. Seay K, Church C, Zheng JH, Deneroff K, Ochsenbauer C, Kappes JC, Liu B, Jeng EK, Wong HC, Goldstein H. 2015. In vivo activation of human NK cells by treatment with an interleukin-15 superagonist potently inhibits acute in vivo HIV-1 infection in humanized mice. J Virol 89:6264–6274. https://doi.org/10.1128/JVI.00563-15.
27. Mohammadi P, Desfarges S, Bartha I, Joos B, Zangger N, Munoz M, Gunthard HF, Beerenwinkel N, Telenti A, Ciuffi A. 2013. 24 hours in the life of HIV-1 in a T cell line. PLoS Pathog 9:e1003161. https://doi.org/10.1371/journal.ppat.1003161.
28. Stratov I, Chung A, Kent SJ. 2008. Robust NK cell-mediated human immunodeficiency virus (HIV)-specific antibody-dependent responses in HIV-infected subjects. J Virol 82:5450–5459. https://doi.org/10.1128/JVI.01952-07.
29. Liu B, Kong L, Han K, Hong H, Marcus WD, Chen X, Jeng EK, Alter S, Zhu X, Rubinstein MP, Shi S, Rhode PR, Cai W, Wong HC. 2016. A novel fusion of ALT-803 (interleukin (IL)-15 superagonist) with an antibody demonstrates antigen-specific antitumor responses. J Biol Chem 291:23869–23881. https://doi.org/10.1074/jbc.M116.733600.
30. Forthal DN, Landucci G, Daar ES. 2001. Antibody from patients with acute human immunodeficiency virus (HIV) infection inhibits primary strains of HIV type 1 in the presence of natural-killer effector cells. J Virol 75:6953–6961. https://doi.org/10.1128/JVI.75.15.6953-6961.2001.
31. Hessell AJ, Hangartner L, Hunter M, Havenith CE, Beurskens FJ, Bakker JM, Lanigan CM, Landucci G, Forthal DN, Parren PW, Marx PA, Burton DR. 2007. Fc receptor but not complement binding is important in antibody protection against HIV. Nature 449:101–104. https://doi.org/10.1038/nature06106.
32. Gooneratne SL, Richard J, Lee WS, Finzi A, Kent SJ, Parsons MS. 2015. Slaying the Trojan horse: natural killer cells exhibit robust anti-HIV-1 antibody-dependent activation and cytolysis against allogeneic T cells. J Virol 89:97–109. https://doi.org/10.1128/JVI.02461-14.
33. Smalls-Mantey A, Doria-Rose N, Klein R, Patamawenu A, Migueles SA, Ko SY, Hallahan CW, Wong H, Liu B, You L, Scheid J, Kappes JC, Ochsenbauer C, Nabel GJ, Mascola JR, Connors M. 2012. Antibody-dependent cellular cytotoxicity against primary HIV-infected CD4+ T cells is directly associated with the magnitude of surface IgG binding. J Virol 86:8672–8680. https://doi.org/10.1128/JVI.00287-12.
34. Bonsignori M, Pollara J, Moody MA, Alpert MD, Chen X, Hwang KK, Gilbert PB, Huang Y, Gurley TC, Kozink DM, Marshall DJ, Whitesides JF, Tsao CY, Kaewkungwal J, Nitayaphan S, Pitisuttithum P, Rerks-Ngarm S, Kim JH, Michael NL, Tomaras GD, Montefiori DC, Lewis GK, DeVico A, Evans DT, Ferrari G, Liao HX, Haynes BF. 2012. Antibody-dependent cellular cytotoxicity-mediating antibodies from an HIV-1 vaccine efficacy trial target multiple epitopes and preferentially use the VH1 gene family. J Virol 86:11521–11532. https://doi.org/10.1128/JVI.01023-12.
35. Ahmad R, Sindhu ST, Toma E, Morisset R, Vincelette J, Menezes J, Ahmad A. 2001. Evidence for a correlation between antibody-dependent cellular cytotoxicity-mediating anti-HIV-1 antibodies and prognostic predictors of HIV infection. J Clin Immunol 21:227–233. https://doi.org/10.1023/A:1011087132180.
36. Baum LL, Cassutt KJ, Knigge K, Khattri R, Margolick J, Rinaldo C, Kleeberger CA, Nishanian P, Henrard DR, Phair J. 1996. HIV-1 gp120-specific antibody-dependent cell-mediated cytotoxicity correlates with rate of disease progression. J Immunol 157:2168–2173.
37. Lambotte O, Ferrari G, Moog C, Yates NL, Liao HX, Parks RJ, Hicks CB, Owzar K, Tomaras GD, Montefiori DC, Haynes BF, Delfraissy JF. 2009. Heterogeneous neutralizing antibody and antibody-dependent cell cytotoxicity responses in HIV-1 elite controllers. AIDS 23:897–906. https://doi.org/10.1097/QAD.0b013e328329f97d.
38. Lewis GK. 2014. Role of Fc-mediated antibody function in protective immunity against HIV-1. Immunology 142:46–57. https://doi.org/10.1111/imm.12232.
39. Chung AW, Isitman G, Navis M, Kramski M, Center RJ, Kent SJ, Stratov I. 2011. Immune escape from HIV-specific antibody-dependent cellular cytotoxicity (ADCC) pressure. Proc Natl Acad Sci U S A 108:7505–7510. https://doi.org/10.1073/pnas.1016048108.
40. Lu CL, Murakowski DK, Bournazos S, Schoofs T, Sarkar D, Halper-Stromberg A, Horwitz JA, Nogueira L, Golijanin J, Gazumyan A, Ravetch JV, Caskey M, Chakraborty AK, Nussenzweig MC. 2016. Enhanced clear-

ance of HIV-1-infected cells by broadly neutralizing antibodies against HIV-1 in vivo. Science 352:1001–1004. https://doi.org/10.1126/science.aaf1279.
41. Kwong PD, Wyatt R, Robinson J, Sweet RW, Sodroski J, Hendrickson WA. 1998. Structure of an HIV gp120 envelope glycoprotein in complex with the CD4 receptor and a neutralizing human antibody. Nature 393:648–659. https://doi.org/10.1038/31405.
42. Asokan M, Rudicell RS, Louder M, McKee K, O'Dell S, Stewart-Jones G, Wang K, Xu L, Chen X, Choe M, Chuang G, Georgiev IS, Joyce MG, Kirys T, Ko S, Pegu A, Shi W, Todd JP, Yang Z, Bailer RT, Rao S, Kwong PD, Nabel GJ, Mascola JR. 2015. Bispecific antibodies targeting different epitopes on the HIV-1 envelope exhibit broad and potent neutralization. J Virol 89:12501–12512. https://doi.org/10.1128/JVI.02097-15.
43. Klein JS, Bjorkman PJ. 2010. Few and far between: how HIV may be evading antibody avidity. PLoS Pathog 6:e1000908. https://doi.org/10.1371/journal.ppat.1000908.
44. Mouquet H, Scheid JF, Zoller MJ, Krogsgaard M, Ott RG, Shukair S, Artyomov MN, Pietzsch J, Connors M, Pereyra F, Walker BD, Ho DD, Wilson PC, Seaman MS, Eisen HN, Chakraborty AK, Hope TJ, Ravetch JV, Wardemann H, Nussenzweig MC. 2010. Polyreactivity increases the apparent affinity of anti-HIV antibodies by heteroligation. Nature 467:591–595. https://doi.org/10.1038/nature09385.
45. Pluckthun A. 2010. HIV: antibodies with a split personality. Nature 467:537–538. https://doi.org/10.1038/467537a.
46. Niwa R, Hatanaka S, Shoji-Hosaka E, Sakurada M, Kobayashi Y, Uehara A, Yokoi H, Nakamura K, Shitara K. 2004. Enhancement of the antibody-dependent cellular cytotoxicity of low-fucose IgG1 Is independent of FcgammaRIIIa functional polymorphism. Clin Cancer Res 10:6248–6255. https://doi.org/10.1158/1078-0432.CCR-04-0850.
47. Bournazos S, Klein F, Pietzsch J, Seaman MS, Nussenzweig MC, Ravetch JV. 2014. Broadly neutralizing anti-HIV-1 antibodies require Fc effector functions for in vivo activity. Cell 158:1243–1253. https://doi.org/10.1016/j.cell.2014.08.023.
48. Barouch DH, Whitney JB, Moldt B, Klein F, Oliveira TY, Liu J, Stephenson KE, Chang HW, Shekhar K, Gupta S, Nkolola JP, Seaman MS, Smith KM, Borducchi EN, Cabral C, Smith JY, Blackmore S, Sanisetty S, Perry JR, Beck M, Lewis MG, Rinaldi W, Chakraborty AK, Poignard P, Nussenzweig MC, Burton DR. 2013. Therapeutic efficacy of potent neutralizing HIV-1-specific monoclonal antibodies in SHIV-infected rhesus monkeys. Nature 503:224–228. https://doi.org/10.1038/nature12744.
49. Halper-Stromberg A, Lu CL, Klein F, Horwitz JA, Bournazos S, Nogueira L, Eisenreich TR, Liu C, Gazumyan A, Schaefer U, Furze RC, Seaman MS, Prinjha R, Tarakhovsky A, Ravetch JV, Nussenzweig MC. 2014. Broadly neutralizing antibodies and viral inducers decrease rebound from HIV-1 latent reservoirs in humanized mice. Cell 158:989–999. https://doi.org/10.1016/j.cell.2014.07.043.
50. Klein F, Halper-Stromberg A, Horwitz JA, Gruell H, Scheid JF, Bournazos S, Mouquet H, Spatz LA, Diskin R, Abadir A, Zang T, Dorner M, Billerbeck E, Labitt RN, Gaebler C, Marcovecchio PM, Incesu RB, Eisenreich TR, Bieniasz PD, Seaman MS, Bjorkman PJ, Ravetch JV, Ploss A, Nussenzweig MC. 2012. HIV therapy by a combination of broadly neutralizing antibodies in humanized mice. Nature 492:118–122. https://doi.org/10.1038/nature11604.
51. Shingai M, Nishimura Y, Klein F, Mouquet H, Donau OK, Plishka R, Buckler-White A, Seaman M, Piatak M, Jr, Lifson JD, Dimitrov DS, Nussenzweig MC, Martin MA. 2013. Antibody-mediated immunotherapy of macaques chronically infected with SHIV suppresses viraemia. Nature 503:277–280. https://doi.org/10.1038/nature12746.
52. Lorenzi JC, Cohen YZ, Cohn LB, Kreider EF, Barton JP, Learn GH, Oliveira T, Lavine CL, Horwitz JA, Settler A, Jankovic M, Seaman MS, Chakraborty AK, Hahn BH, Caskey M, Nussenzweig MC. 2016. Paired quantitative and qualitative assessment of the replication-competent HIV-1 reservoir and comparison with integrated proviral DNA. Proc Natl Acad Sci U S A 113:E7908–E7916. https://doi.org/10.1073/pnas.1617789113.
53. Caskey M, Klein F, Nussenzweig MC. 2016. Broadly neutralizing antibodies for HIV-1 prevention or immunotherapy. N Engl J Med 375:2019–2021. https://doi.org/10.1056/NEJMp1613362.
54. Caskey M, Schoofs T, Gruell H, Settler A, Karagounis T, Kreider EF, Murrell B, Pfeifer N, Nogueira L, Oliveira TY, Learn GH, Cohen YZ, Lehmann C, Gillor D, Shimeliovich I, Unson-O'Brien C, Weiland D, Robles A, Kummerle T, Wyen C, Levin R, Witmer-Pack M, Eren K, Ignacio C, Kiss S, West AP, Jr, Mouquet H, Zingman BS, Gulick RM, Keler T, Bjorkman PJ, Seaman MS, Hahn BH, Fatkenheuer G, Schlesinger SJ, Nussenzweig MC, Klein F. 2017. Antibody 10-1074 suppresses viremia in HIV-1-infected individuals. Nat Med https://doi.org/10.1038/nm.4268.
55. Guo D, Shi X, Arledge KC, Song D, Jiang L, Fu L, Gong X, Zhang S, Wang X, Zhang L. 2012. A single residue within the V5 region of HIV-1 envelope facilitates viral escape from the broadly neutralizing monoclonal antibody VRC01. J Biol Chem 287:43170–43179. https://doi.org/10.1074/jbc.M112.399402.
56. Lynch RM, Wong P, Tran L, O'Dell S, Nason MC, Li Y, Wu X, Mascola JR. 2015. HIV-1 fitness cost associated with escape from the VRC01 class of CD4 binding site neutralizing antibodies. J Virol 89:4201–4213. https://doi.org/10.1128/JVI.03608-14.
57. Chen W, Xiao X, Wang Y, Zhu Z, Dimitrov DS. 2010. Bifunctional fusion proteins of the human engineered antibody domain m36 with human soluble CD4 are potent inhibitors of diverse HIV-1 isolates. Antiviral Res 88:107–115. https://doi.org/10.1016/j.antiviral.2010.08.004.
58. Richard J, Veillette M, Brassard N, Iyer SS, Roger M, Martin L, Pazgier M, Schon A, Freire E, Routy JP, Smith AB 3rd, Park J, Jones DM, Courter JR, Melillo BN, Kaufmann DE, Hahn BH, Permar SR, Haynes BF, Madani N, Sodroski JG, Finzi A. 2015. CD4 mimetics sensitize HIV-1-infected cells to ADCC. Proc Natl Acad Sci U S A 112:E2687–E2694. https://doi.org/10.1073/pnas.1506755112.
59. Bolton DL, Pegu A, Wang K, McGinnis K, Nason M, Foulds K, Letukas V, Schmidt SD, Chen X, Todd JP, Lifson JD, Rao S, Michael NL, Robb ML, Mascola JR, Koup RA. 2015. Human immunodeficiency virus type 1 monoclonal antibodies suppress acute simian-human immunodeficiency virus viremia and limit seeding of cell-associated viral reservoirs. J Virol 90:1321–1332. https://doi.org/10.1128/JVI.02454-15.
60. Trist HM, Tan PS, Wines BD, Ramsland PA, Orlowski E, Stubbs J, Gardiner EE, Pietersz GA, Kent SJ, Stratov I, Burton DR, Hogarth PM. 2014. Polymorphisms and interspecies differences of the activating and inhibitory FcgammaRII of Macaca nemestrina influence the binding of human IgG subclasses. J Immunol 192:792–803. https://doi.org/10.4049/jimmunol.1301554.
61. Davis SJ, Ward HA, Puklavec MJ, Willis AC, Williams AF, Barclay AN. 1990. High level expression in Chinese hamster ovary cells of soluble forms of CD4 T lymphocyte glycoprotein including glycosylation variants. J Biol Chem 265:10410–10418.
62. Edmonds TG, Ding H, Yuan X, Wei Q, Smith KS, Conway JA, Wieczorek L, Brown B, Polonis V, West JT, Montefiori DC, Kappes JC, Ochsenbauer C. 2010. Replication competent molecular clones of HIV-1 expressing Renilla luciferase facilitate the analysis of antibody inhibition in PBMC. Virology 408:1–13. https://doi.org/10.1016/j.virol.2010.08.028.
63. Seay K, Khajoueinejad N, Zheng JH, Kiser P, Ochsenbauer C, Kappes JC, Herold B, Goldstein H. 2015. The vaginal acquisition and dissemination of HIV-1 infection in a novel transgenic mouse model is facilitated by coinfection with herpes simplex virus 2 and is inhibited by microbicide treatment. J Virol 89:9559–9570. https://doi.org/10.1128/JVI.01326-15.
64. Miyawaki A. 2007. Bringing bioluminescence into the picture. Nat Methods 4:616–617. https://doi.org/10.1038/nmeth0807-616.
65. Joseph A, Zheng JH, Follenzi A, Dilorenzo T, Sango K, Hyman J, Chen K, Piechocka-Trocha A, Brander C, Hooijberg E, Vignali DA, Walker BD, Goldstein H. 2008. Lentiviral vectors encoding human immunodeficiency virus type 1 (HIV-1)-specific T-cell receptor genes efficiently convert peripheral blood CD8 T lymphocytes into cytotoxic T lymphocytes with potent in vitro and in vivo HIV-1-specific inhibitory activity. J Virol 82:3078–3089. https://doi.org/10.1128/JVI.01812-07.
66. Ying T, Du L, Ju TW, Prabakaran P, Lau CC, Lu L, Liu Q, Wang L, Feng Y, Wang Y, Zheng BJ, Yuen KY, Jiang S, Dimitrov DS. 2014. Exceptionally potent neutralization of Middle East respiratory syndrome coronavirus by human monoclonal antibodies. J Virol 88:7796–7805. https://doi.org/10.1128/JVI.00912-14.
67. Montefiori DC. 2009. Measuring HIV neutralization in a luciferase reporter gene assay. Methods Mol Biol 485:395–405. https://doi.org/10.1007/978-1-59745-170-3_26.
68. Hessell AJ, Jaworski JP, Epson E, Matsuda K, Pandey S, Kahl C, Reed J, Sutton WF, Hammond KB, Cheever TA, Barnette PT, Legasse AW, Planer S, Stanton JJ, Pegu A, Chen X, Wang K, Siess D, Burke D, Park BS, Axthelm MK, Lewis A, Hirsch VM, Graham BS, Mascola JR, Sacha JB, Haigwood NL. 2016. Early short-term treatment with neutralizing human monoclonal antibodies halts SHIV infection in infant macaques. Nat Med 22:362–368. https://doi.org/10.1038/nm.4063.